Original Paper

A Numerical Analysis for Vibration Behaviors of a Crankshaft with a Shear Rubber Torsional Damper

By Kunio Shimoyamada*, Tomoaki Kodama**, Yasuhiro Honda***,
Katsuhiko Wakabayashi****, and Shoichi Iwamoto*****

Synopsis: This paper refers to a numerical computation for vibration displacements and stresses of a crankshaft with a shear type rubber torsional damper by the three dimensional transfer matrix method.

In this work, the numerical computation method is proposed to compute the vibration displacements and stresses by means of replacing the rubber part of rubber torsional damper with a spring-dashpot model. Then dynamic characteristics are estimated by the complex torsional stiffness derived from a three-element Maxwell model. As a result the torsional vibration stress and bending vibration stress and vibration displacements (angular and lateral displacements) can be computed with an adequate accuracy.

1. introduction

The increased output and lighter weight of the high-speed automotive diesel engine have resulted in loss of rigidity in the crankshaft. As a result, torsional vibration, bending vibration and a combination of these two vibrations have occurred on the crankshaft system. These cause vibrations and noises due to torsional vibration displacement and stress. In order to reduce the vibrations and noises, the shear type rubber torsional damper (rubber damper) has been generally used[1)~3),6),7)].

Theoretical vibration analyses and their application to high-speed diesel engine crankshaft have been reported with regard to torsional angular displacement and stress and bending vibration stress[5),8)~18)].

Then, in this work, in order to establish the optimum design of crankshaft, a numerical computation method by the three dimensional transfer matrix method is proposed to compute the torsional vibration displacement and stress of a crankshaft with rubber damper for Vee type 8-cylinder diesel engine. In modeling the whole crankshaft system for numerical computation, the rubber part of rubber damper is replaced with a spring-dashpot model. Then dynamic characteristic values are estimated by complex torsional stiffness derived from a three-element Maxwell model. The accuracy of this numerical computation method is confirmed by comparing computed results with measured ones.

---

*Associate Professor, Department of Mechanical Engineering
**Technical Staff, Department of Mechanical Engineering
***Associate Professor, Department of Mechanical Engineering, Dr. of Engineering
****Professor, Department of Mechanical Engineering, Dr. of Engineering
*****Professor, Department of Mechanical Engineering, Saitama University, Dr. of Engineering

2. Definition of Symbols

This section defines symbols used in this work.

Section Forces and Displacements

M_x : Torsional moment [Nm]
M_y, M_z : Bending moments around y- and z-axis, respectively [Nm]
N : Force in the x-axis direction [N]
Q : Shearing force in the z-axis direction [N]
V : Shearing force in the y-axis direction [N]
u : Displacement in the x-axis direction [m]
v, w : Deflection in the y- and z-axis direction, respectively [m]
θ : Crank rotation angle [rad]
θ_x : Torsional angle [rad]
θ_y, θ_z : Deflection angle around y- and z-axis, respectively [rad]

Matrixes and Vectors

$\boldsymbol{Z}_{P1}$, $\boldsymbol{Z}_{P2}$: Square transfer matrix, crank pin
$\boldsymbol{Z}_{PC}$: Square transfer matrix, fillet of crank pin
$\boldsymbol{Z}_{AM1,i}$, $\boldsymbol{Z}_{AM2,i}$: Square transfer matrix, i-th rigid element of crank arm
$\boldsymbol{Z}_{AE1,i}$, $\boldsymbol{Z}_{AE2,i}$: Square transfer matrix, i-th elastic element of crank arm
$\boldsymbol{Z}_{J}$: Square transfer matrix, journal shaft
$\boldsymbol{Z}_{JC}$: Square transfer matrix, fillet of journal
$\boldsymbol{Z}_{PU}$: Square transfer matrix, pulley
$\boldsymbol{Z}_{FL}$: Square transfer matrix, flywheel
$\boldsymbol{Z}_{J,R,i}$: Square transfer matrix, i-th right hand side element of crankshaft
$\boldsymbol{Z}_{J,L,i}$: Square transfer matrix, i-th left hand side element of crankshaft
$\boldsymbol{Z}_{PHAS1}$, $\boldsymbol{Z}_{PHAS2}$: Square transfer matrix, coordinate conversion between member coordinate systems
$\boldsymbol{Z}_{PH}$: Square transfer matrix, phase change between adjacent throws
$\boldsymbol{Z}_{F}$: Square transfer matrix, external force
$\boldsymbol{Z}_{K,i}$: Square transfer matrix, i-th main bearing
$\boldsymbol{Z}_{L}$: Square transfer matrix, thrust bearing
$\boldsymbol{Z}$: Square transfer matrix, whole crankshaft system of engine
$\boldsymbol{Z}_{ED}$: Square transfer matrix, eddy-current dynamometer
$\boldsymbol{Z}_{EDJ,L,i}$: Square transfer matrix, i-th left hand side element of dynamometer
$\boldsymbol{Z}_{EDK}$: Square transfer matrix, bearing of dynamometer
$\boldsymbol{Z}_{EDR}$: Square transfer matrix, rotor of dynamometer
$\boldsymbol{Z}_{EDJ,R,i}$: Square transfer matrix, i-th right hand side element of dynamometer
$\boldsymbol{Z}_{AIS}$: Square transfer matrix, intermediate shaft
$\boldsymbol{Z}_{PL}$: Square transfer matrix, plate
$\boldsymbol{Z}_{E}$: Square transfer matrix, engine
$\boldsymbol{Z}_{RDI}$: Square transfer matrix, inertia ring of rubber damper
$\boldsymbol{Z}_{RDR}$: Square transfer matrix, rubber part of rubber damper
$\boldsymbol{Z}_{RDH}$: Square transfer matrix, housing of rubber damper
$\boldsymbol{Z}_{RD}$: Square transfer matrix, rubber damper
$\boldsymbol{q}$: Column vector, state vector
$\boldsymbol{q}_{RD,R}$: Column vector, state vector at right hand side of rubber damper
$\boldsymbol{q}_{RD,L}$: Column vector, state vector at left hand side of rubber damper
$\boldsymbol{q}_{RD,R}$: Column vector, state vector at right hand side of eddy-current dynamometer
$\boldsymbol{q}_{PU,L}$: Column vector, state vector at left hand side of pulley

Others

K^* : Complex torsional stiffness [Nm/rad]
K_d : Dynamic torsional stiffness [Nm/rad]
C_d : Damping coefficient [Nms]

K_1, K_2, τ_1 : Element values of three-element Maxwell model
ω : Angular frequency [rad/s]

3. Specification of Test Engine and Rubber Damper

Specifications of the Vee-8 cylinder diesel engine and test rubber damper on which this work is based are listed in Table 1 and Table 2, respectively.

The shape and dimensions of test rubber damper are illustrated in Fig. 1. This rubber damper is usually used by connecting to the test engine and natural rubber is used for the rubber part of rubber damper.

Table 1 Specifications of test engine

Items		Contents
Type of engine		Direct injection diesel water-cooled, 4 stroke cycle
Number of cylinders		8-cylinder
Arrangement		90 Vee
Bore and stroke	m	0.135 x 0.125
Total stroke volume	m^3	0.0143
Compression ratio		16.0
Type of cooling		Forced water-cooling
Maximum output	kW/r/min	206 / 2500
Maximum torque	Nm/r/min	863 / 1400
Firing order		1R-1L-4R-4L-3L-2R-2L-3R
Gross weight [dry]	Kg	107

Table 2 Specifications of test rubber damper

Items		Values
Inertia moment of inertia ring	Kgm^2	0.156
Weight of inertia ring	Kg	0.855
Inertia moment of housing	Kgm^2	0.363
Weight of housing	Kg	0.248

4. Derivation of Dynamic Characteristics by Three-Element Maxwell Model[19)~21)]

The three-element Maxwell model was adopted to estimate the dynamic characteristics of rubber part of rubber damper in this work. The equilibrium differential equation in three-element Maxwell model as shown in Fig. 2 can be represented as follows;

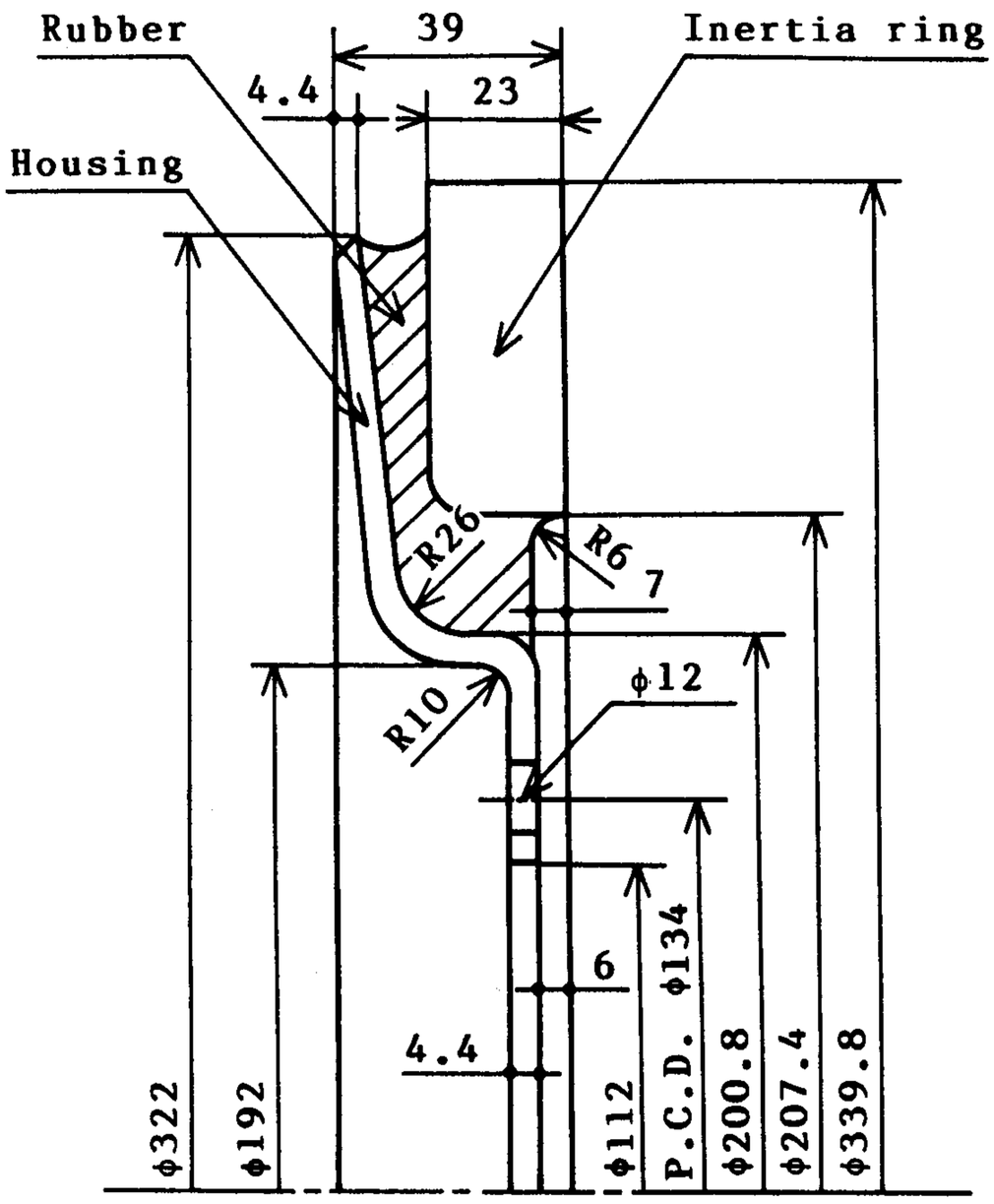

Fig. 1 Shape and dimensions of test rubber damper

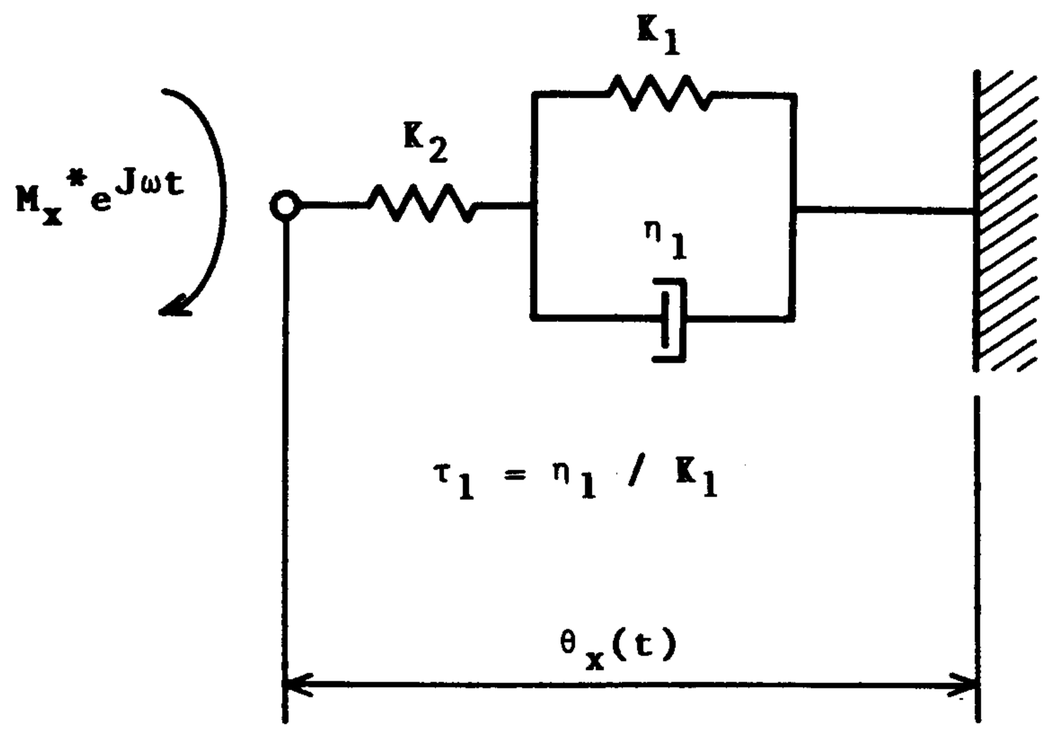

Fig. 2 Three-element Maxwell model

$$\frac{dM_x}{dt}+\frac{1}{\tau_1}\left(1+\frac{K_2}{K_1}\right)M_x=K_2\frac{d\theta_x}{dt}+\frac{K_2}{\tau_1} \tag{1}$$

Solving equation (1) with respect to time t and rearranging for $\theta_x(t)$, the general solution can be obtained as follows;

$$\theta_x(t)=\left[\frac{1}{K_2}+\frac{1}{K_1(K_1+j\omega\tau_1)}\right]\cdot M_x^* \exp(j\omega t) \tag{2}$$

Assuming $\theta_x(t)=\theta_x^* \exp(j\omega t)$, the complex torsional stiffness $K^*(\omega)$ can be obtained as follows;

$$K^*(\omega)=\frac{K_1K_2[K_1+\omega^2\tau_1^2]+K_2}{(K_1+K_2)^2+K_1^2\omega^2\tau_1^2} \tag{3}$$

and dynamic torsional stiffness K_d and damping coefficient C_d can be represented by separating equation (3) into real and imaginary parts as follows,

$$K_d(\omega)=\frac{K_1K_2[K_1+\omega^2\tau_1^2]+K_2}{(K_1+K_2)^2+K_1^2\omega^2\tau_1^2} \tag{4}$$

$$C_d(\omega)=\frac{K_1K_2\tau_1}{(K_1+K_2)^2+K_1^2\omega^2\tau_1^2} \tag{5}$$

The dynamic characteristic values can be calculated by substituting element values of Maxwell model into equations (4) and (5).

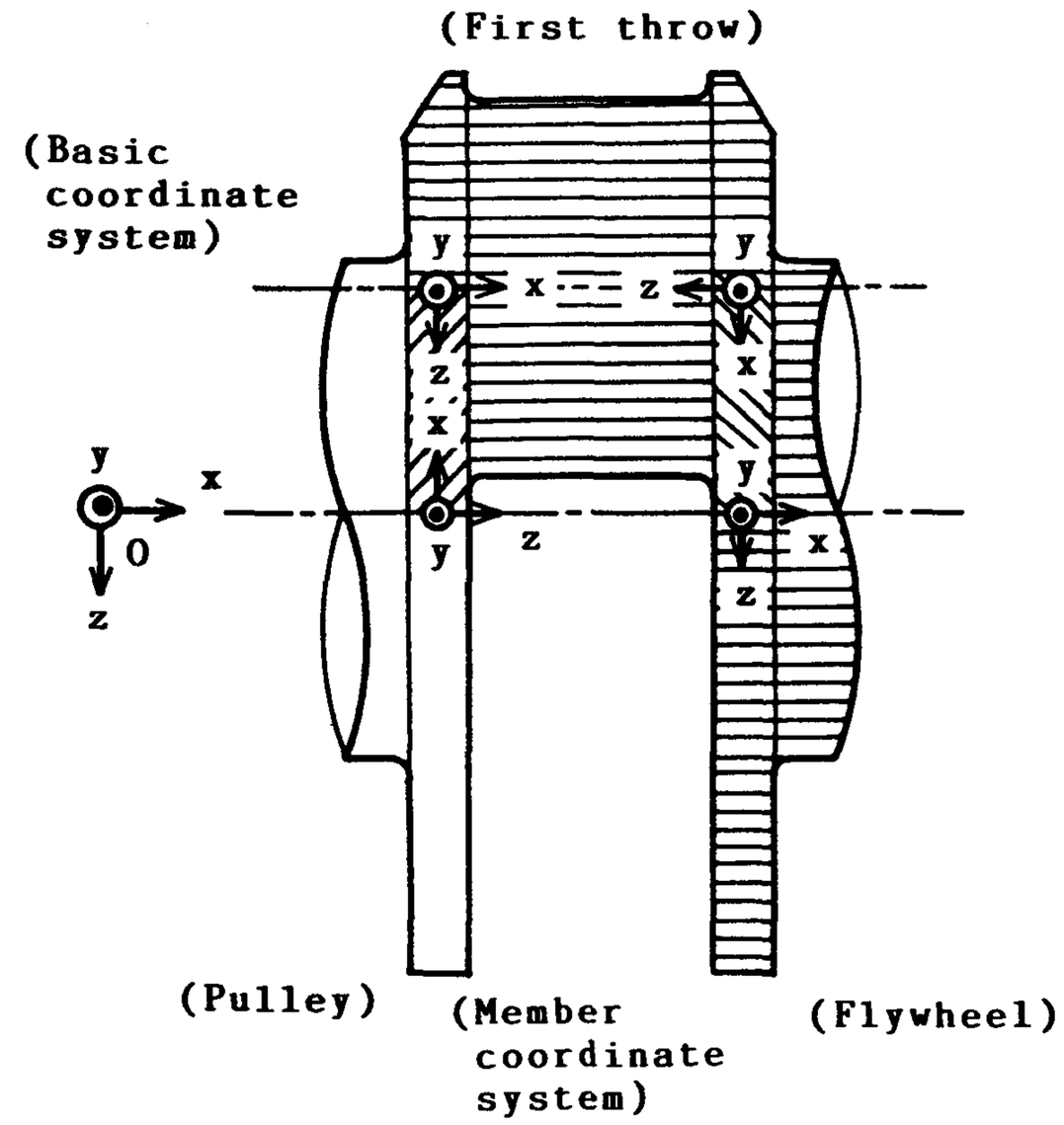

Fig. 3 Relationship between standard and local coordinate system

5. A Numerical Computation Method for Torsional Vibration Stress and Displacement by Three Dimensional Transfer Matrix Method[8)~11),18)~21)]

The numerical computation by three dimensional transfer matrix method is described for computing the torsional vibration stress and displacement for a Vee type 8-cylinder diesel engine.

5.1 Definition of State Vector and Coordinate System

The coordinate system is defined as shown in Fig. 3, as a standard right-hand coordinate system with the origin on the axis of revolution of the front end of the crankshaft (the end opposite the flywheel), and local right-hand coordinate systems with respect to each element of the crankshaft, virtually divided into elements for numerical computation according to its shape. The standard and local coordinate systems are defined in a certain relationship to each other.

The state vector q is defined as equation (6). This state vector consists of 13 physical quantities including a unit component which is used to introduce external forces.

$$q=[u, N, \theta_x, M_x, v, \theta_z, M_z, V, w, \theta_y, M_y, Q, 1]^T \quad (T\text{: transposition}) \qquad (6)$$

5.2 Vibration Model of a Vee, 8-Cylinder Diesel Engine Crankshaft, the Detailed *i*-th Crank Throw and Rubber Damper

The whole vibration model of crankshaft system on which this numerical computation method is based is illustrated in Fig. 4.

A crankshaft is to be elastically supported by main bearing and thrust bearing and to be subjected to external forces at each crank pin. In modeling for most of the numerical computation method, the main bearig and thrust bearing are assumed to be approximately

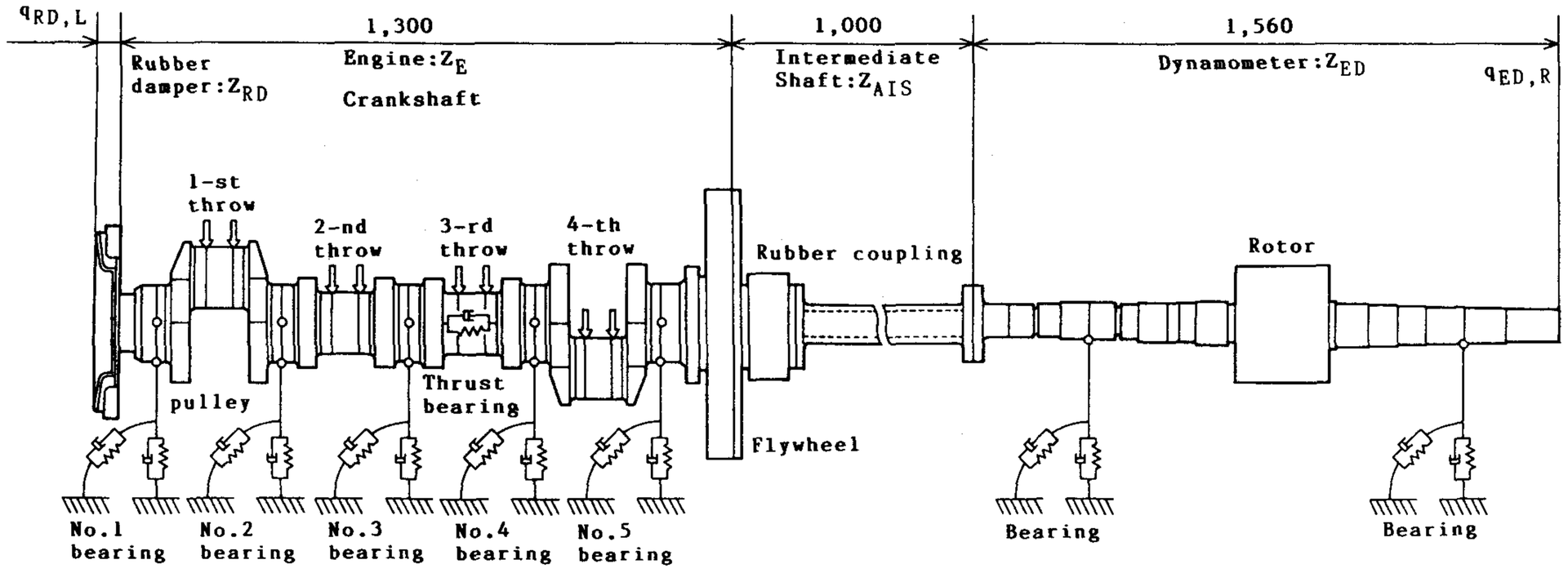

Fig. 4 Whole vibration model of a Vee 8-cylinder engine crankshaft for transfer matrix method

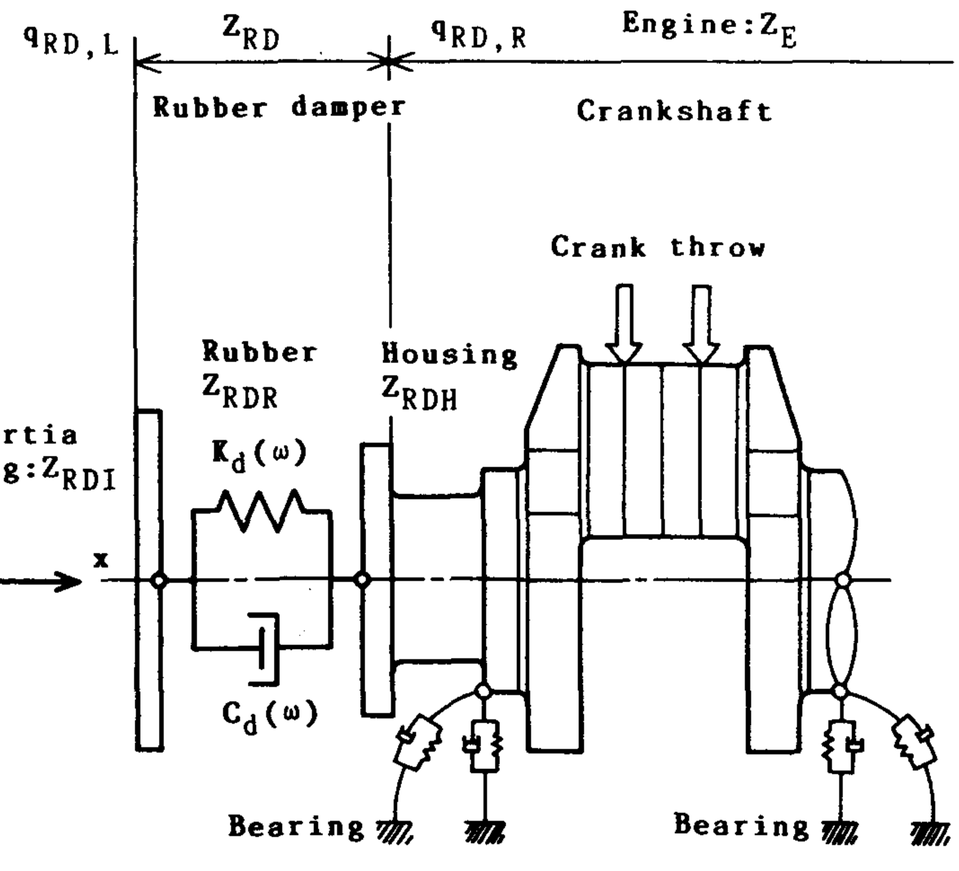

Fig. 5 Vibration model of crankshaft with a rubber damper for transfer matrix method

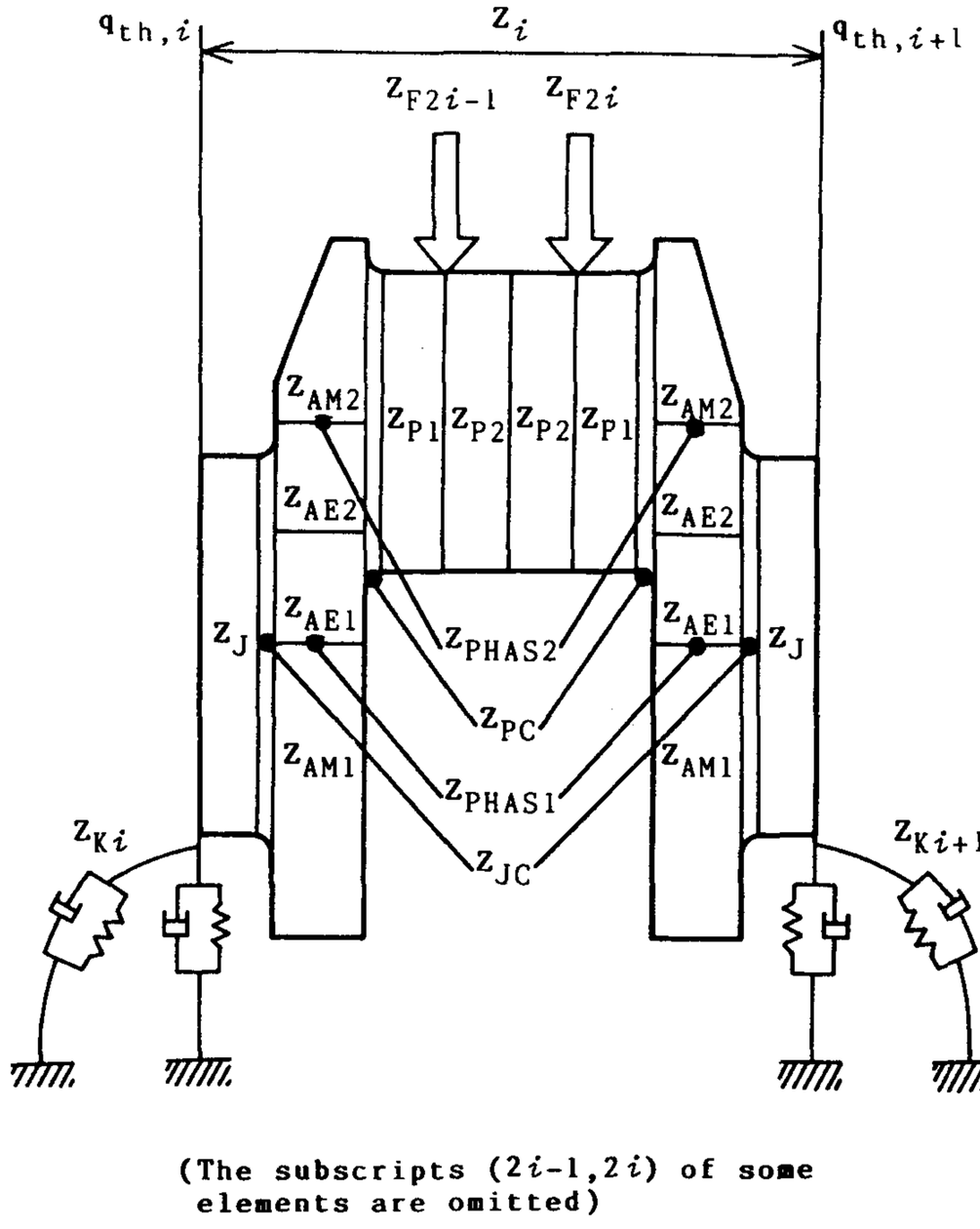

Fig. 6 Detailed vibration model of *i*-th crank throw for transfer matrix method

replaced with concentrated equivalent linear spring and damping. The external forces of Vee type diesel engine are applied in concentration to two divided sections on each crank pin [See Fig. 4].

Fig. 5 shows a vibration model of rubber damper for numerical computation. K_d and C_d in the figure are calculated by equations (4) and (5), and these values are used to compute numerically the rubber part of rubber damper.

Fig. 6 shows a detailed vibration model of the *i*-th crank throw. Moreover, the phase difference of the crank throw due to the shape of the crankshaft is considered at the left

hand side of each crank throw.

In order to apply the transfer matrix method, transfer matrices for each element of crankshaft are derived by mass-elastic and rigid body element system, and transfer matrices for the change of coordinate systems must be considered at four points of each crank throw [See Fig. 2].

5.3 Transfer Equation and Numerical Matrix Solution

After the transfer matrices for the above-mentioned elements are all specified, these transfer matrices are connected regularly from left hand side to the right hand side. Transfer equation of i-th crank throw can be represented as follows.

$$\begin{aligned} \boldsymbol{Z}_i = & \boldsymbol{Z}_{\mathrm{J},\,i+1}\boldsymbol{Z}_{\mathrm{JC},\,i+1}\boldsymbol{Z}_{\mathrm{AM1},\,2i}\boldsymbol{Z}_{\mathrm{PHAS1},\,2i}\boldsymbol{Z}_{\mathrm{AE1},\,2i}\boldsymbol{Z}_{\mathrm{AE2},\,2i} \\ & \cdot \boldsymbol{Z}_{\mathrm{PHAS2},\,2i}\boldsymbol{Z}_{\mathrm{AM2},\,2i}\boldsymbol{Z}_{\mathrm{PC},\,i}\boldsymbol{Z}_{\mathrm{P1},\,i}\boldsymbol{Z}_{\mathrm{F},\,2i}\boldsymbol{Z}_{\mathrm{P2},\,i}\boldsymbol{Z}_{\mathrm{P2},\,i}\boldsymbol{Z}_{\mathrm{F},\,2i-1} \\ & \cdot \boldsymbol{Z}_{\mathrm{P1},\,i}\boldsymbol{Z}_{\mathrm{PC},\,i}\boldsymbol{Z}_{\mathrm{AM2},\,2i-1}\boldsymbol{Z}_{\mathrm{PHAS2},\,2i-1}\boldsymbol{Z}_{\mathrm{AE2},\,2i-1} \\ & \cdot \boldsymbol{Z}_{\mathrm{AE1},\,2i-1}\boldsymbol{Z}_{\mathrm{PHAS1},\,2i-1}\boldsymbol{Z}_{\mathrm{AM1},\,2i-1}\boldsymbol{Z}_{\mathrm{JC},\,i}\boldsymbol{Z}_{\mathrm{J},\,i}\boldsymbol{Z}_{\mathrm{K},\,i}\boldsymbol{Z}_{\mathrm{PH},\,i} \end{aligned} \tag{7}$$

Next, from the vibration model for rubber damper shown in Fig. 5, the transfer equation connecting state vector $\boldsymbol{q}_{\mathrm{RD,\,L}}$ at the left hand side of the rubber damper and state vector $\boldsymbol{q}_{\mathrm{RD,\,R}}$ at right hand side of the rubber damper can be represented by the following equation (8).

$$\boldsymbol{q}_{\mathrm{RD,\,R}} = \boldsymbol{Z}_{\mathrm{RDH}}\boldsymbol{Z}_{\mathrm{RDR}}\boldsymbol{Z}_{\mathrm{RDI}}\boldsymbol{q}_{\mathrm{RD,\,L}} = \boldsymbol{Z}_{\mathrm{RD}} \cdot \boldsymbol{q}_{\mathrm{RD,\,L}} \tag{8}$$

Applying the equation (4) and (5), the transfer matrix $\boldsymbol{Z}_{\mathrm{RDR}}$ of the rubber part [See Fig. 5] is represented by the following equation (9). In this case, for simplicity, the equation (9) is represented by physical quantities θ_{x} and M_{x} of state vector only.

$$\begin{aligned} \begin{bmatrix} \theta_{\mathrm{x}} \\ M_{\mathrm{x}} \\ 1 \end{bmatrix}_{\mathrm{RDR,\,R}} &= \begin{bmatrix} 1 & -\dfrac{K_{\mathrm{d}}}{K_{\mathrm{d}}^2+C_{\mathrm{d}}^2\cdot\omega^2}+j\dfrac{C_{\mathrm{d}}\cdot\omega}{K_{\mathrm{d}}^2+C_{\mathrm{d}}^2\cdot\omega^2} & 0 \\ 0 & 1 & 0 \\ 0 & 0 & 1 \end{bmatrix} \cdot \begin{bmatrix} \theta_{\mathrm{x}} \\ M_{\mathrm{x}} \\ 1 \end{bmatrix}_{\mathrm{RDR,\,L}} \\ &= \boldsymbol{Z}_{\mathrm{RDR}} \cdot \begin{bmatrix} \theta_{\mathrm{x}} \\ M_{\mathrm{x}} \\ 1 \end{bmatrix}_{\mathrm{RDR,\,L}} \end{aligned} \tag{9}$$

Finally, from the vibration model for the whole crankshaft system shown in Fig. 4, the transfer equation connecting state vector $\boldsymbol{q}_{\mathrm{RD,\,L}}$ at the left hand side of the rubber damper and state vector $\boldsymbol{q}_{\mathrm{RD,\,R}}$ at the right hand side of the dynamometer can be represented by the following equation (10),

$$\boldsymbol{q}_{\mathrm{ED,\,R}} = \boldsymbol{Z}_{\mathrm{ED}}\boldsymbol{Z}_{\mathrm{AIS}}\boldsymbol{Z}_{\mathrm{E}}\boldsymbol{Z}_{\mathrm{RD}}\boldsymbol{q}_{\mathrm{RD,\,L}} = \boldsymbol{Z} \cdot \boldsymbol{q}_{\mathrm{RD,\,L}} \tag{10}$$

where,

$$\boldsymbol{Z}_{\mathrm{E}} = \boldsymbol{Z}_{\mathrm{FL}}\boldsymbol{Z}_{\mathrm{J,\,R,\,2}}\boldsymbol{Z}_{\mathrm{J,\,R,\,1}}\boldsymbol{Z}_{\mathrm{K,\,5}}\boldsymbol{Z}_{\mathrm{PH,\,5}}\boldsymbol{Z}_{4}\boldsymbol{Z}_{3}\boldsymbol{Z}_{\mathrm{L,\,Z2}}\boldsymbol{Z}_{1}\boldsymbol{Z}_{\mathrm{J,\,L,\,2}}\boldsymbol{Z}_{\mathrm{J,\,L,\,1}}\boldsymbol{Z}_{\mathrm{PU}} \tag{11}$$

$$\boldsymbol{Z}_{\mathrm{AIS}} = \boldsymbol{Z}_{\mathrm{IS}}\boldsymbol{Z}_{\mathrm{RC}}\boldsymbol{Z}_{\mathrm{PL}} \tag{12}$$

$$\boldsymbol{Z}_{\mathrm{ED}} = \boldsymbol{Z}_{\mathrm{EDJ,\,R,\,2}}\boldsymbol{Z}_{\mathrm{EDK,\,2}}\boldsymbol{Z}_{\mathrm{EDJ,\,R,\,1}}\boldsymbol{Z}_{\mathrm{ED,\,R}}\boldsymbol{Z}_{\mathrm{EDJ,\,L,\,2}}\boldsymbol{Z}_{\mathrm{EDK,\,1}}\boldsymbol{Z}_{\mathrm{EDJ,\,L,\,1}} \tag{13}$$

Since the boundary conditions at both left and right hand sides are free, these boundary conditions are applied to equation (10). All forces and moments are zero and displacement is

an unknown. Therefore, the boundary matrix $\boldsymbol{R}_L$ and the unknown displacement vector $\boldsymbol{A}_L$ are introduced to derive the physical quantities. The state vector at the left hand side of crankshaft under boundary cnditions can be represented as follows,

$$\boldsymbol{q}_{RD,L}=\boldsymbol{R}_L\boldsymbol{A}_L$$

therefore, equation (10) can be represented by equation (14).

$$\boldsymbol{q}_{ED,R}=\boldsymbol{Z}\boldsymbol{q}_{RD,L}=\boldsymbol{Z}\boldsymbol{R}_L\boldsymbol{A}_L \tag{14}$$

Also, assuming a free end at the right hand side of crankshaft system, boundary matrix $\boldsymbol{R}_R$ is introduced to derive the physical quantities and premultiplied by state vector $\boldsymbol{q}_{ED,R}$ at the right hand side of crankshaft system, so it is shown that,

$$\boldsymbol{O}=\boldsymbol{R}_R\boldsymbol{q}_{ED,R} \tag{15}$$

Therefore, from equation (13) and equation (14), it is shown that,

$$\boldsymbol{R}_R\boldsymbol{Z}\boldsymbol{R}_L\boldsymbol{A}_L=\boldsymbol{O} \tag{16}$$

By solving a set of complex linear equation, the unkown displacement $\boldsymbol{A}_L$ at left hand side of rubber damper can be determined. The state vectors at each arbitrary divided position are obtained by premultiplying successively the obtained state vector $\boldsymbol{q}_{RD,L}$ at the left hand side by the transfer matrices. This numerical method can compute the vibration conditions per order by using amplitudes and phase angles of harmonic exciting forces and phase angle of firing order.

6. Measurement of Torsional Vibration Angular Displacement and Stress[4)]

Fig. 7 shows the schematic diagram for measurement of crankshaft vibrations. Engine tests were carried out to measure the waveforms of torsional angular displacement and torsional stress. The test engine was operated with full load from 800 r/min to 2,200 r/min, and the temperature of the rubber part of rubber damper in experiment was held constant.

Torsional augular displacement is measured by torsional angle converter by means of making the gear for measurement at housing and inertia ring of rubber damper. The measured signals are temporarily stored in micro computer and are analyzed by F.F.T. analyzer.

Torsional vibration stress can be obtained through a slip ring from electrical signals of strain gauges attached on the outer sueface of each crank pin. This stress is calculated by the strains apparing on two active gauges at each measuring position. Fig. 8 shows the attached positions of the gauges.

7. Comparison and Investigation of Numerical Computed and Measured Angular Vibration

7.1 On Torsional Angular Displacement

Fig. 9 shows the amplitude of torsional angular displacement obtained from measured result at pulley. Values are shown for 4-th, 7-th, 8-th and 9-th order torsional vibration components with resonant phenomena in operated revolution.

The amplitudes of 7-th and 9-th order torsional vibration components are small because

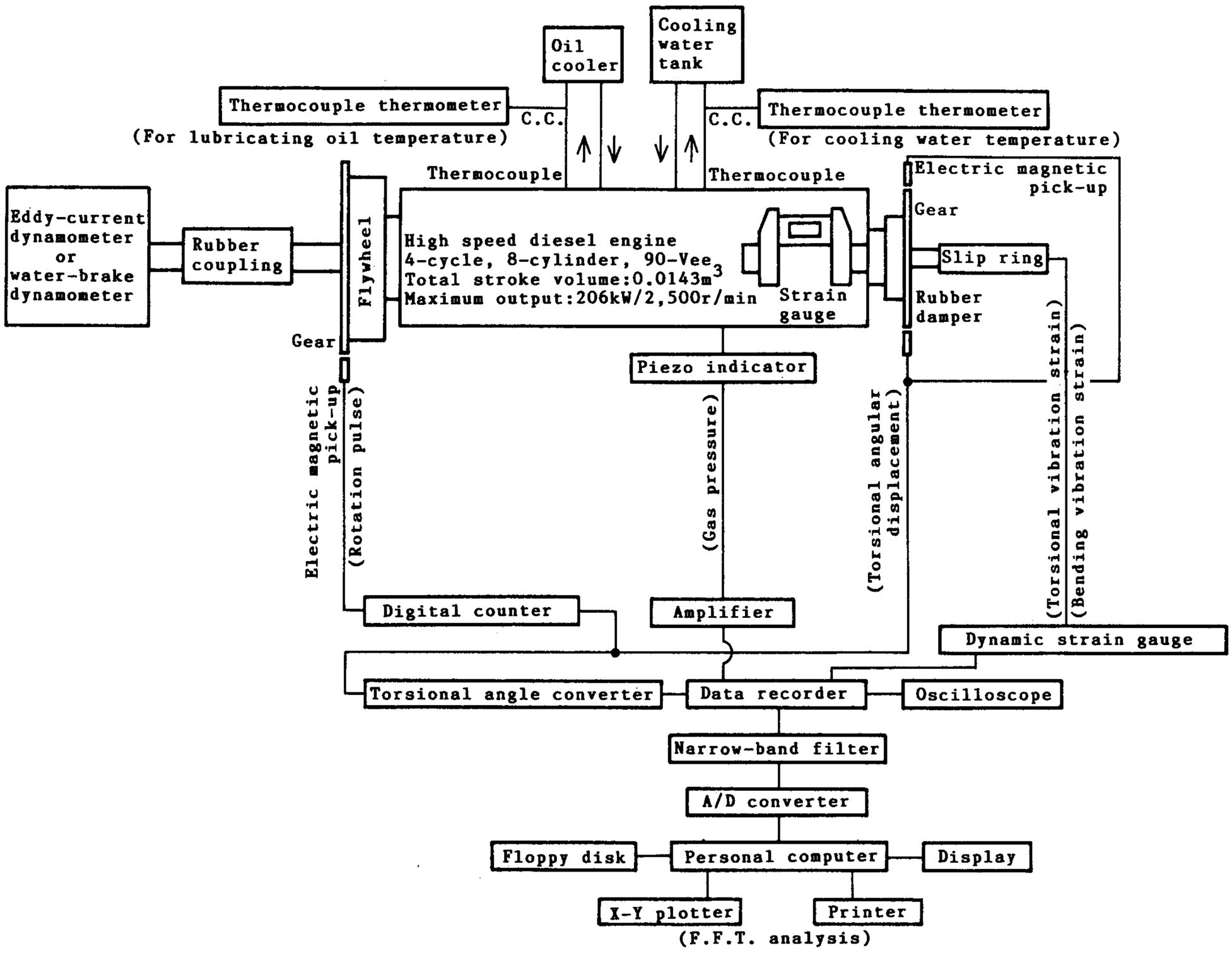

Fig. 7 Schematic diagram for vibration measurement of crankshaft system

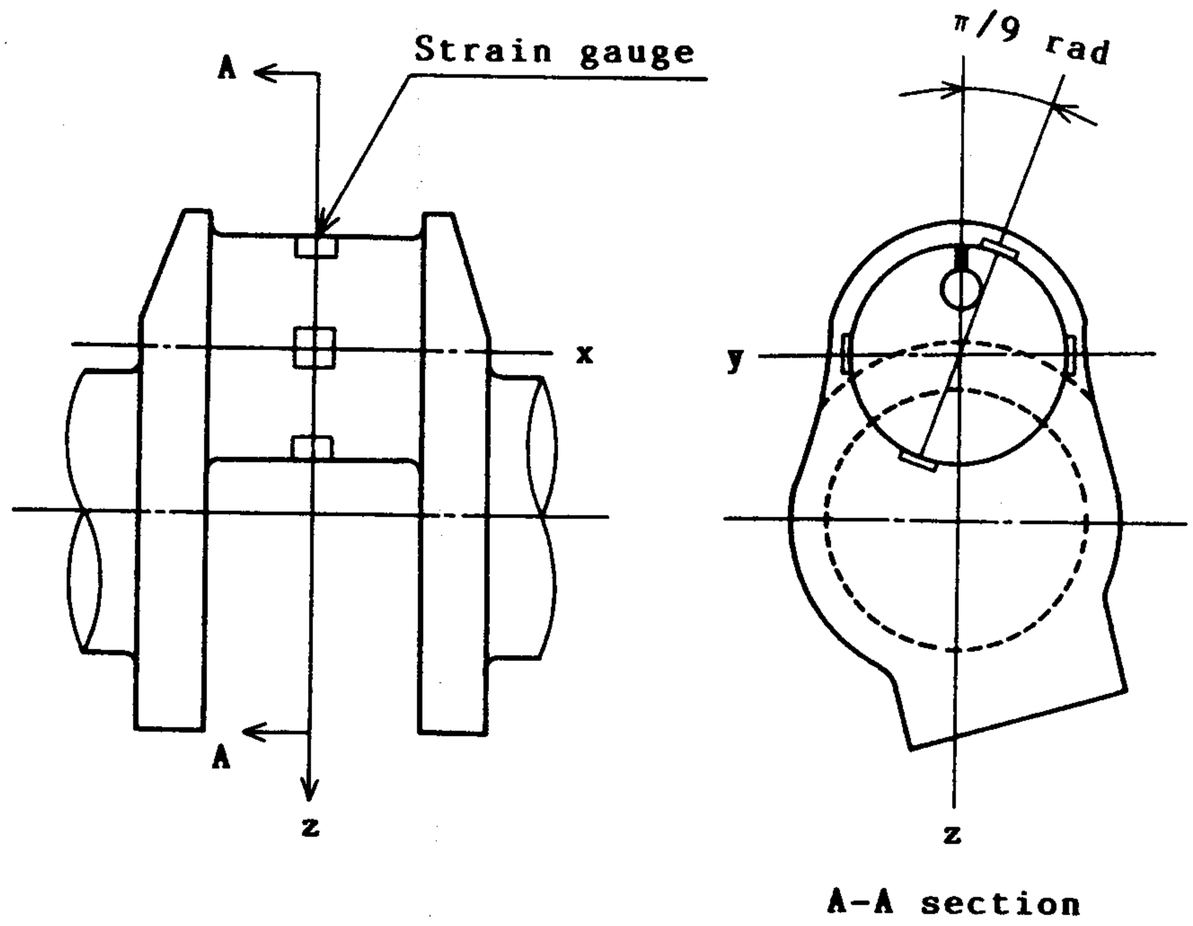

Fig. 8 Adhesived location of strain gauge at crank pin center

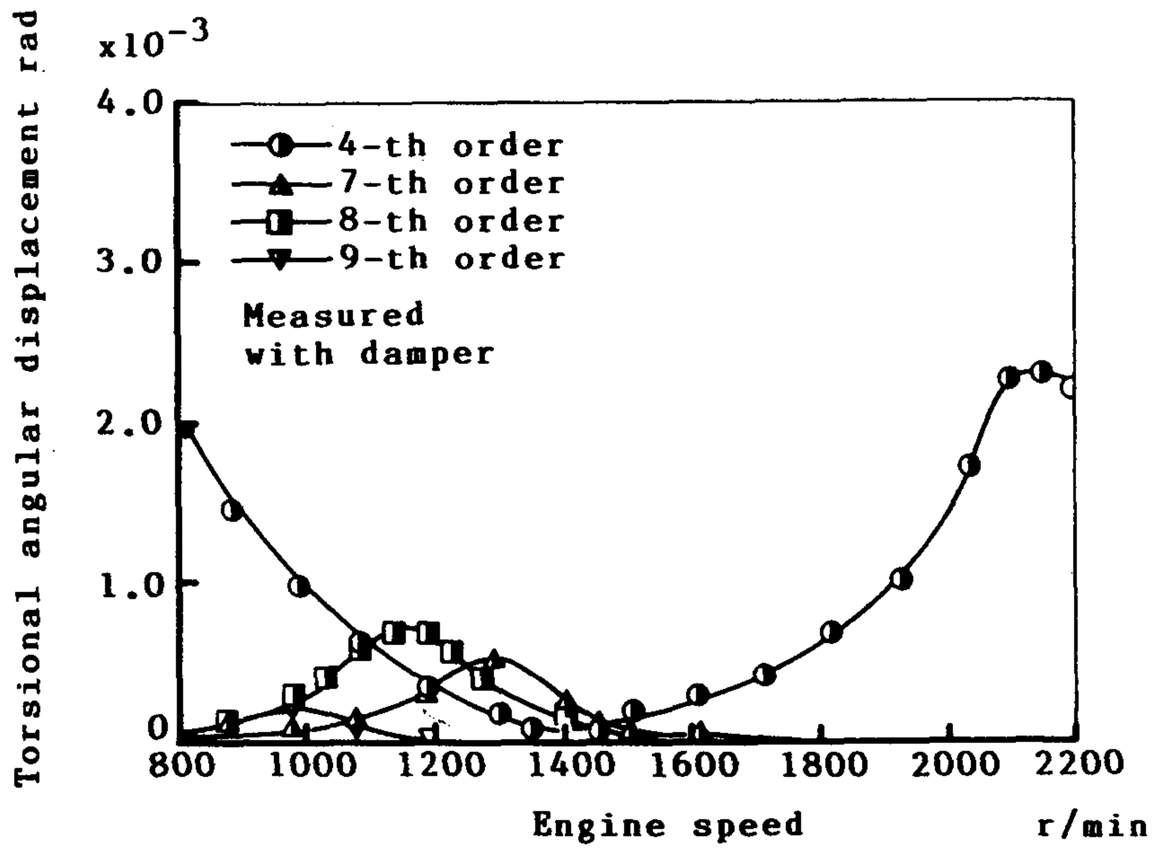

Fig. 9 Amplitude curves of torsional angular displacement at pulley end (with damper, measured)

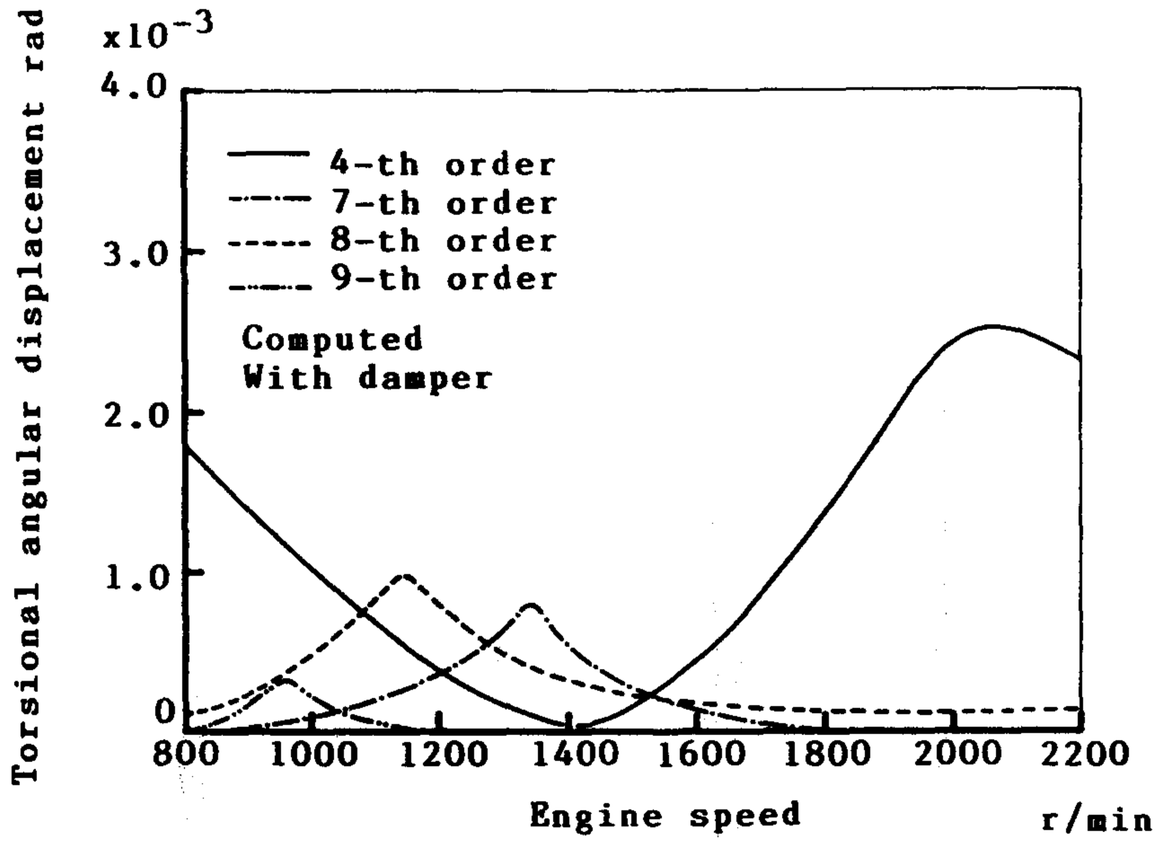

Fig. 10 Amplitude curves of torsional angular displacemment at pulley end (with damper, computed)

the exciting torque is small. By connecting the rubber damper to pulley, the amplitude of the most remarkable 8-th order vibration was reduced below 1/3. The amplitudes of 7-th and 9-th order vibration components are also reduced below 1/2 and 1/3, respectively, but the resonant phenomenon of 4-th order vibration component appears at the neighborhood of 2,110 r/min in operated revolution by means of connecting the rubber damper, so that amplitude is the largest.

In the crankshaft system with rubber damper, the eigen value of engine calculated from each of order vibrations has a small difference. It is considered that this is caused by change of dynamic characteristics of rubber part of rubber damper.

Fig. 10 shows the amplitudes of torsional angular displacement obtained from numerical computation. The computed amplitudes of each order vibration coincide with the measured one. It can be seen that, if the dynamic characteristics of rubber damper are estimated correctly, the previous-mentioned numerical computation method is usable to

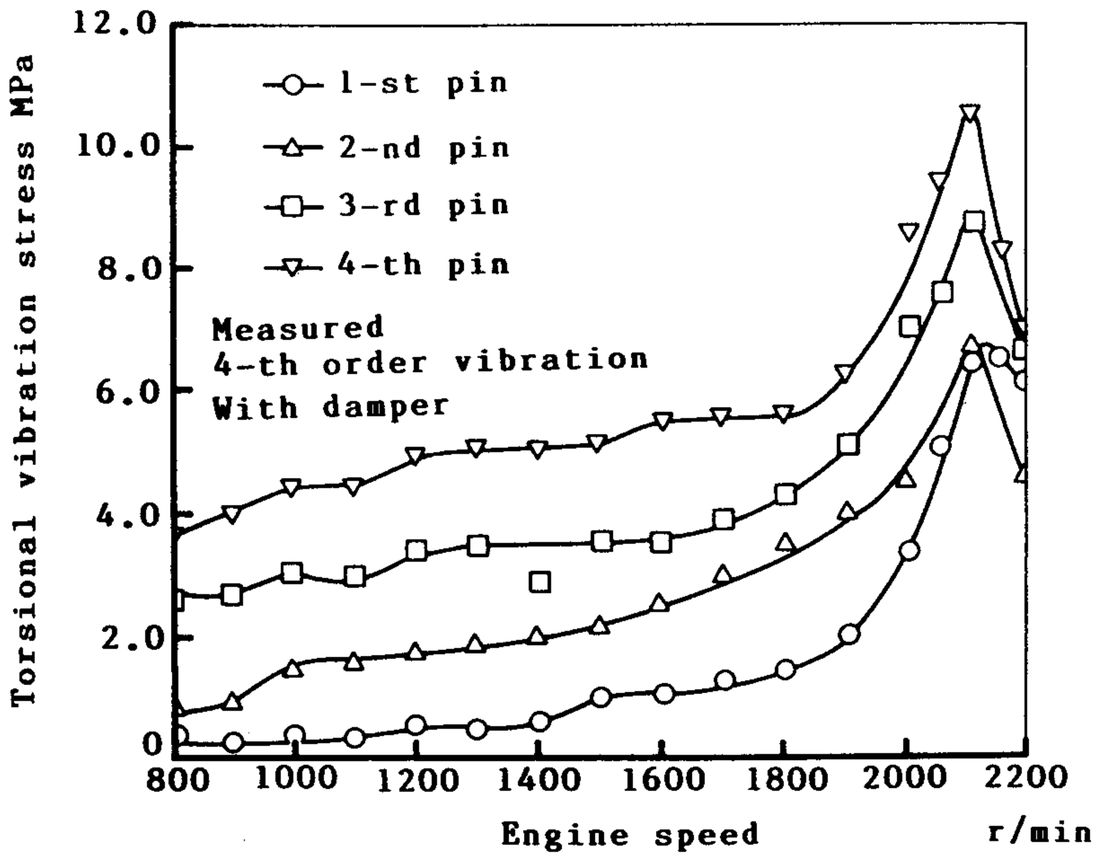

Fig. 11 Amplitude curves of torsional vibration stress at crank pin center (with damper, 4-th order vibration, measured)

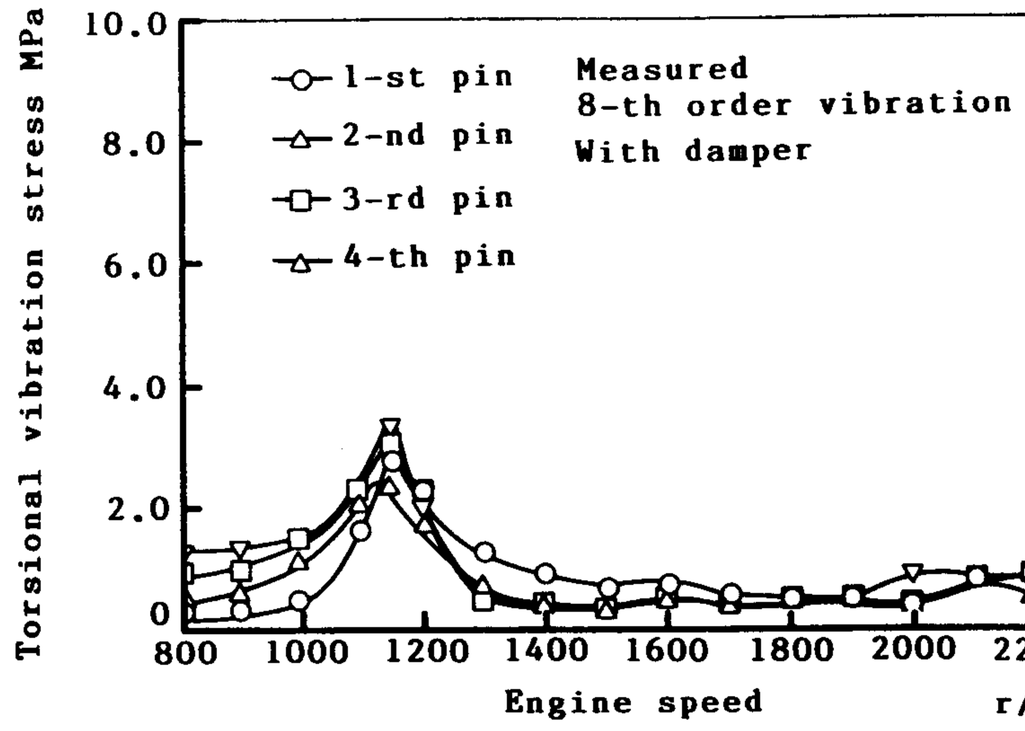

Fig. 12 Amplitude curves of torsional vibration stress at crank pin center (with damper, 8-th order vibration. measured)

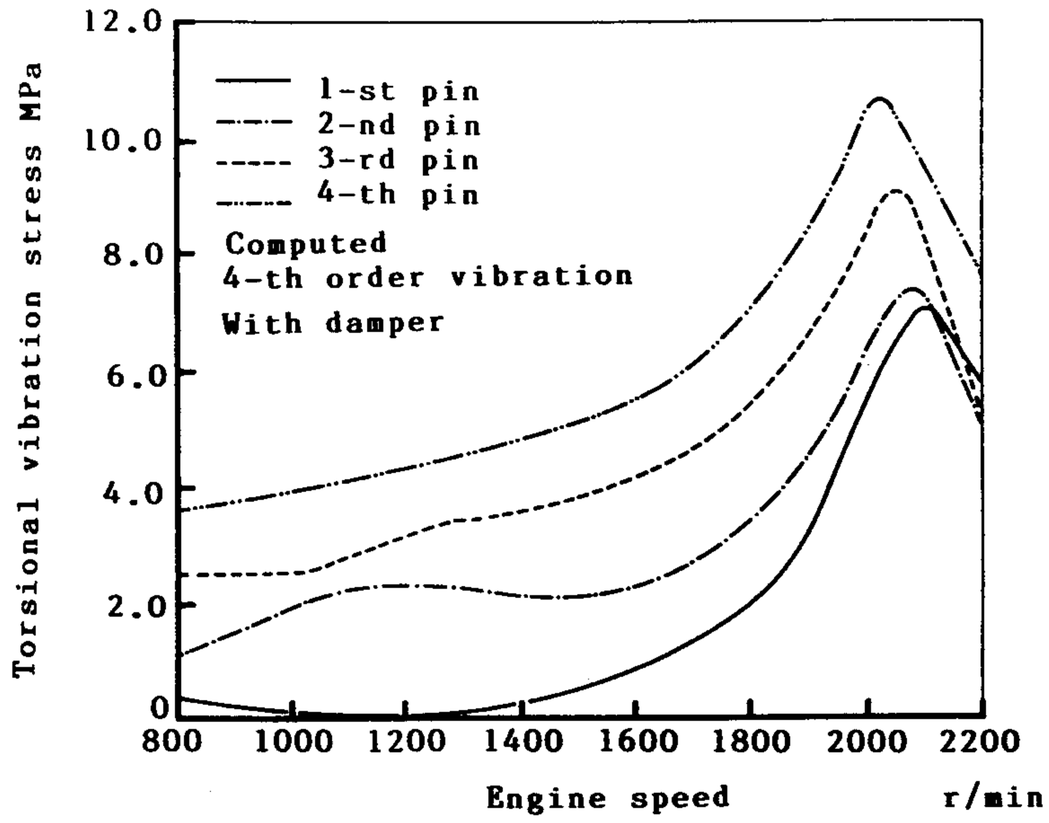

Fig. 13 Amplitude curves of torsional vibration stress at crank pin center (with damper, 4-th order vibration, computed)

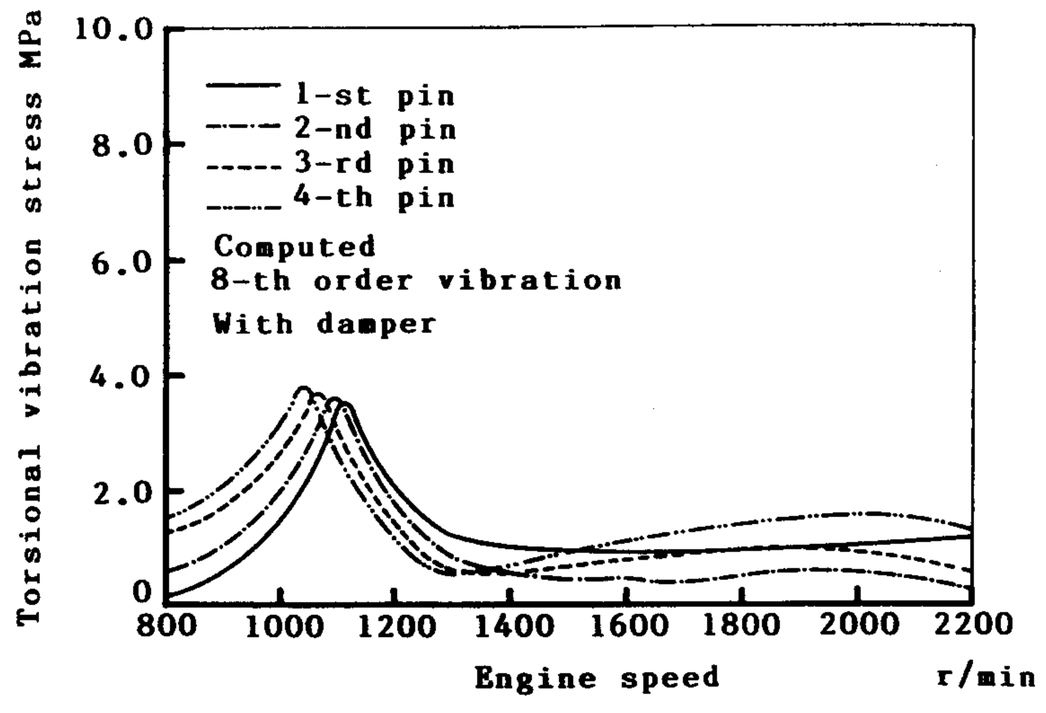

Fig. 14 Amplitude curves of torsional vibration stress at crank pin center (with damper, 8-th order vibration, computed)

compute the torsional vibration displacement.

7.2 On Torsional Vibration Stress

Fig. 11 and Fig. 12 show the measured amplitudes of torsional vibration stress of each midpoint crank pin (1-st pin to 4-th pin numbered from damper side) of crankshaft system with rubber damper. The maximum amplitude values of torsional vibration stress occur in the neighborhood of the resonant revolution of torsional angular displacement. The amplitude values of torsional vibration stress show different stress values due to each crank pin, and these values become larger according to side of the flywheel. The maximum stress values of both order vibration components occur at 4-th crank pin and are 10.7 MPa and 3.8 MPa, respectively.

Fig. 13 and Fig. 14 show the amplitude curves of torsional vibration stress obtained by this numerical computation. Both the amplitude curves of 4-th and 8-th order vibration components coincide with the measured ones. In addition, it has been assured that the torsional vibration displacement and stress can be computed with adequate acceracy by considering the rubber part of rubber damper with such a simple model as shown in Fig. 5.

7.3 Comparison of Maximum Values of Torsional Angular Displacement and Stresses at Resonant Revolution

The maximum amplitude values of torsional vibration displacement and stresses obtained from measured and computed results are compared and listed in Table 3 and Table 4.

8. Investigations of Torsional Vibration and Torsional Moment Modes

In this section, using the physical quantities θ_x and M_x of state vector obtained from the numerical computation, the conditions of torsional vibration and torsional moment of the crankshaft system are investigated by means of illustrating the mode diagrams.

Fig. 15 shows the torsional vibration mode of crankshaft system without rubber damper. Fig. 16 and Fig. 17 show the modes of 4-th and 8-th torsional vibration at the neighborhood of resonant revolutions, respectively. From the mode diagrams, the difference of phase angle between inertia ring and housing is large, and therefore it can not

Table 3(a) Comparison of the computed value with the measured torsional angular displacement (without damper) [No. 1]

Order vibration		Computed value	Measured value
4-th	Resonant engine speed r/min	----	----
	Torsional angular displacement rad	----	----
7-th	Resonant engine speed r/min	1810	1815
	Torsional angular displacement rad	1.42	1.18
8-th	Resonant engine speed r/min	1580	1555
	Torsional angular displacement rad	2.66	2.50
9-th	Resonant engine speed r/min	1368	1400
	Torsional angular displacement rad	0.62	0.62

Table 3(b) Comparison of the computed value with the measured torsional angular displacement (with damper) [No. 2]

Order vibration		Computed value	Measured value
4-th	Resonant engine speed r/min	2058	2128
	Torsional angular displacement rad	2.54	2.30
7-th	Resonant engine speed r/min	1338	1293
	Torsional angular displacement rad	0.79	0.53
8-th	Resonant engine speed r/min	1142	1152
	Torsional angular displacement rad	0.99	0.73
9-th	Resonant engine speed r/min	961	976
	Torsional angular displacement rad	0.32	0.22

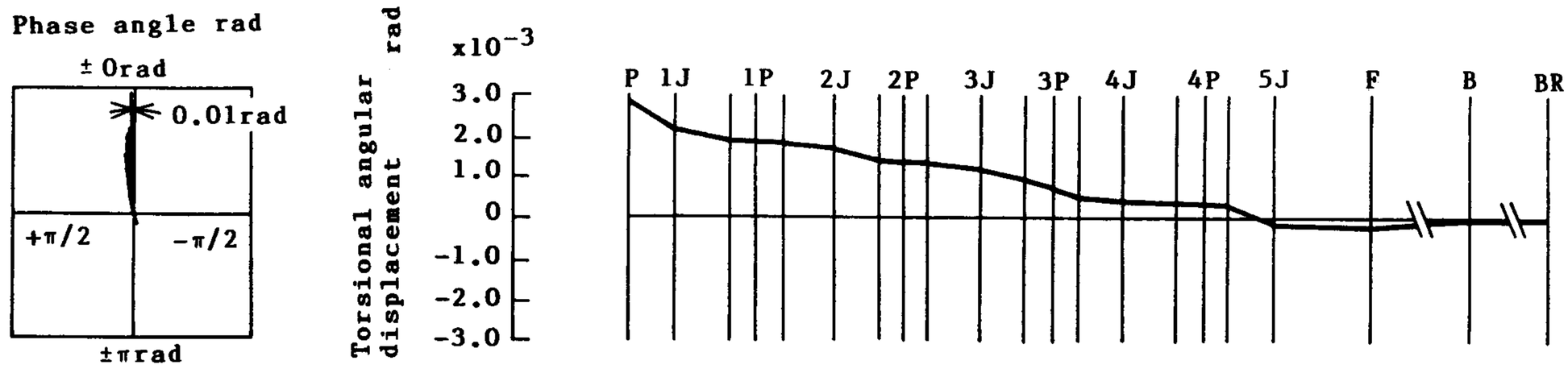

Fig. 15 Vibration mode of torsional angular displacement (without damper, 8-th order vibration, resonant engine speed 1,580 r/min)

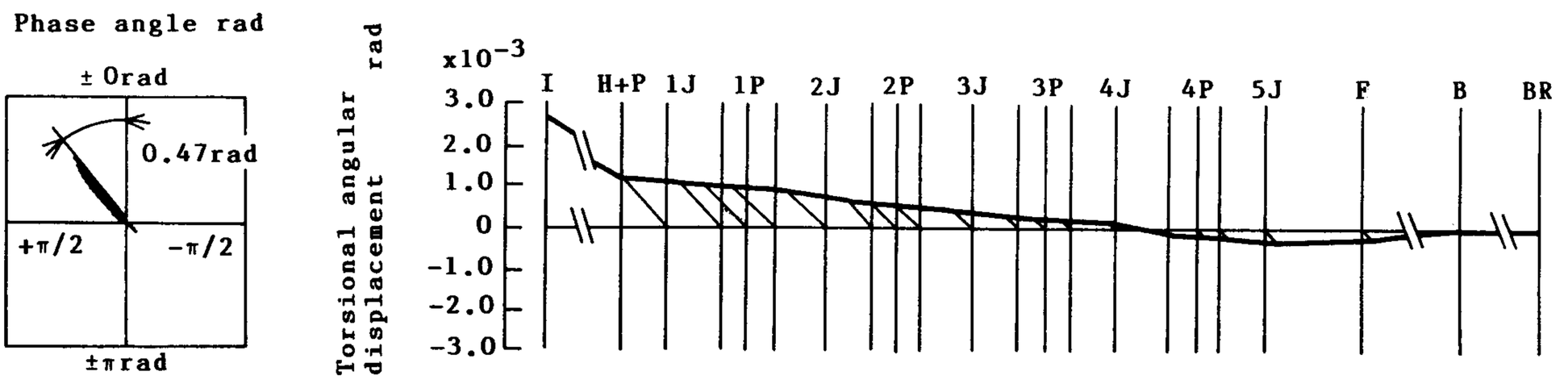

Fig. 16 Vibration mode of torsional angular displacement (with damper, 4-th order vibration, resonant engine speed 2,110 r/min)

Table 4(a) Comparison of the computed value with the measured torsional vibration stress (without damper) [No. 1]

Items		4-th order vibration		8-th order vibration	
		Computed value	Measured value	Computed value	Measured value
1-st Center pin	Resonant engine speed r/min	----	----	1535	1569
	Maximum amplitude MPa	----	----	7.85	6.50
2-nd Center pin	Resonant engine speed r/min	----	----	1531	1565
	Maximum amplitude MPa	----	----	9.55	8.75
3-rd Center pin	Resonant engine speed r/min	----	----	1527	1562
	Maximum amplitude MPa	----	----	11.05	9.44
4-th Center pin	Resonant engine speed r/min	----	----	1523	1558
	Maximum amplitude MPa	----	----	11.91	11.12

Table 4(b) Comparison of the computed value with the measured torsional vibration stress (with damper) [No. 2]

Items		4-th order vibration		8-th order vibration	
		Computed value	Measured value	Computed value	Measured value
1-st Center pin	Resonant engine speed r/min	2098	2133	1115	1142
	Maximum amplitude MPa	7.07	6.79	3.50	2.77
2-nd Center pin	Resonant engine speed r/min	2076	2111	1092	1117
	Maximum amplitude MPa	7.40	6.69	3.57	2.42
3-rd Center pin	Resonant engine speed r/min	2045	2106	1064	1137
	Maximum amplitude MPa	9.11	8.70	3.70	3.02
4-th Center pin	Resonant engine speed r/min	2020	2106	1039	1142
	Maximum amplitude MPa	10.72	10.47	3.77	3.37

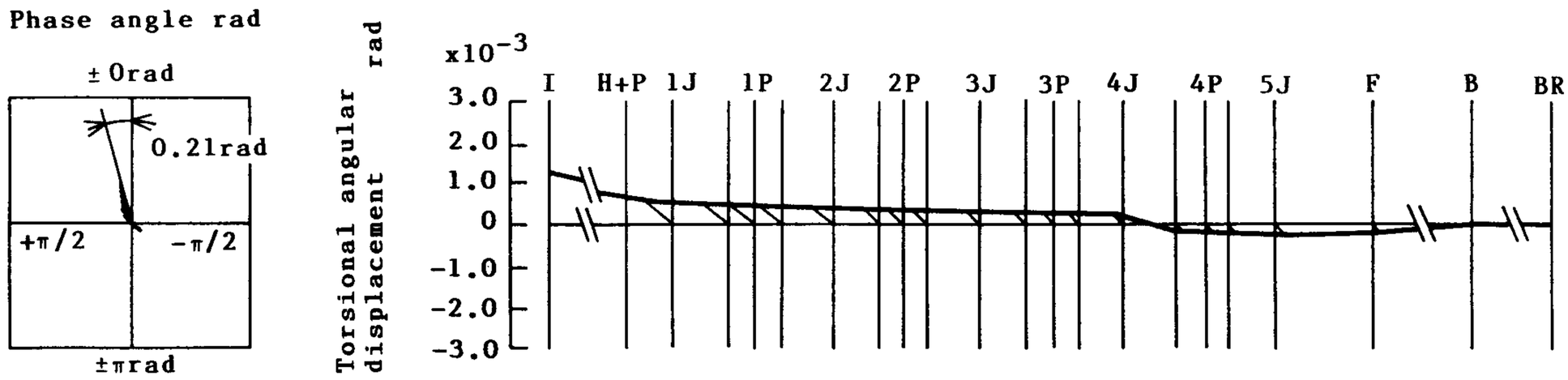

Fig. 17 Vibration mode of torsional angular displacement (with damper, 8-th order vibration, resonant engine speed 1,100 r/min)

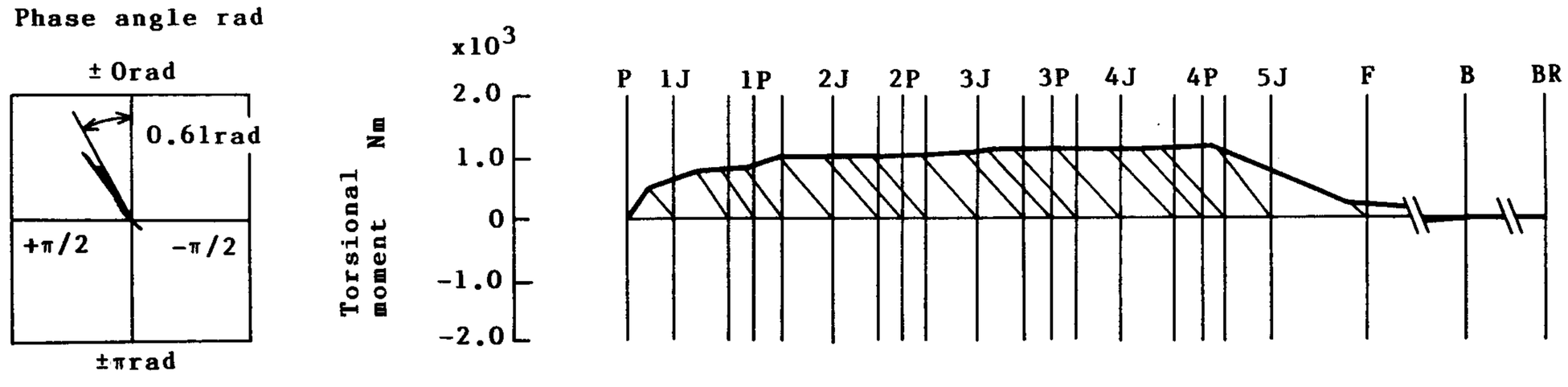

Fig. 18 Vibration mode of torsional moment (without damper, 8-th order vibration, resonant engine speed 1,523 r/min)

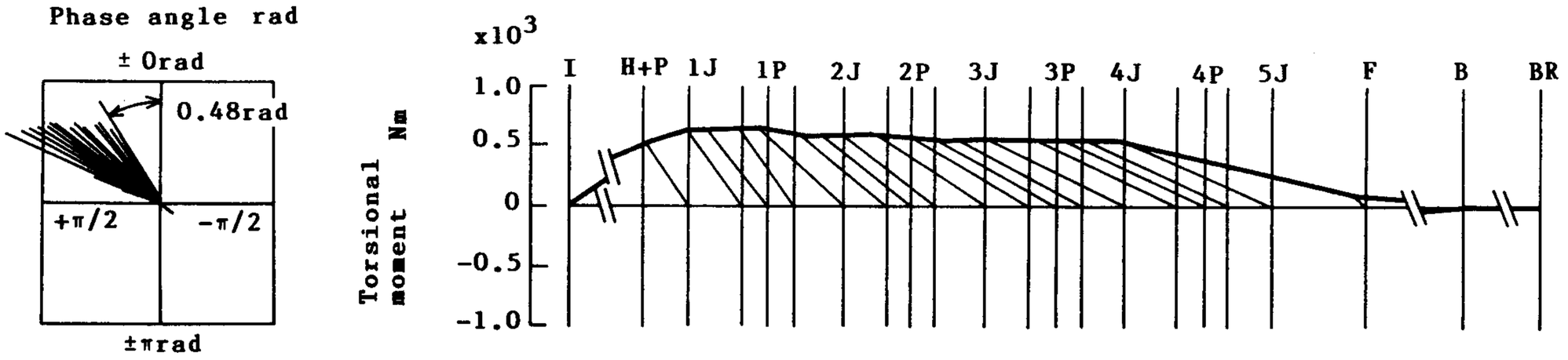

Fig. 19 Vibration mode of torsional moment (with damper, 4-th order vibration, resonant engine speed 2,020 r/min)

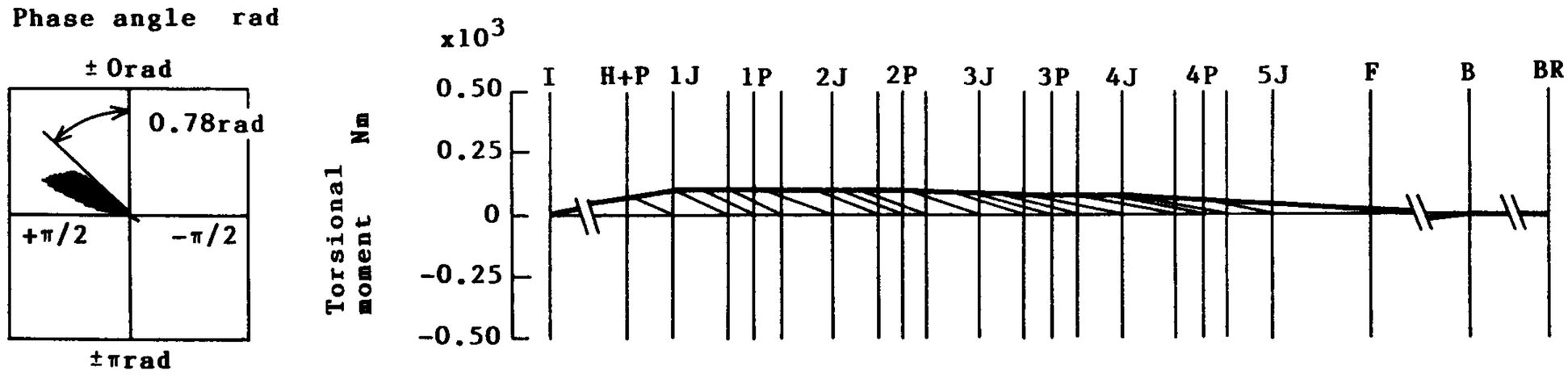

Fig. 20 Vibration mode of torsional moment (with damper, 8-th order vibration, resonant engine speed 1,039 r/min)

be ignored. Comparing Fig. 15 with Fig. 16 or Fig. 17, the vibration node at the neighborhood of 5-th journal of the crankshaft system without a rubber damper moves to the neighborhood of the 4-th journal by means of attaching the rubber damper at pulley.

Fig. 19 and Fig. 20 show the modes of 4-th and 8-th order torsional moments. The maximum torsional moment as shown in Fig. 19 (4-th order vibration) occurs at left hand side of 4-th crank pin. In Fig. 20 (8-th order vibration), it occurs at mid point of 4-th crank pin. Comparing the difference of phase angle btween inertia ring and housing of rubber damper shows that it is large. Therefore, note that the phase angle difference of adjacent positions on crankshaft are also large in comparison with the phase angle differences on crankshaft without rubber damper as shown in Fig. 18.

Applying this numerical computation method, it is seen that the position of order vibration node can be confirmed more exactly.

In Fig. 15 throught 20, notation D denotes the inertia ring of rubber damper, H+P: housing and pulley, 1J to 5J: number of journal, 1P to 4P: number of crank pin, F: Flywheel, B: rotor of dynamometer and BR: right side of dynamometer.

9. Consideration and Investigations

9.1 On Lateral Displacement at Pulley

Lateral displacement amplitudes at pulley of the crankshaft system are represented by using numerically computed results. The lateral displacement amplitudes represented in this section include the amplitudes of both bending vibration and torsional-bending coupled vibration (coupled bending vibration) displacements.

Fig. 21 and Fig. 22 show the amplitudes of lateral displacements in the y- and z-direction of 4-th and 8-th order torsional vibration components at pulley.

In 8-th order vibration component as shown in Fig. 22, the amplitude values of lateral displacements are small in comparison with those of 4-th order vibration component. It is considered that the lateral displacement due to bending vibration is more influenced by the coupled bending vibration.

Especially, in the crankshaft system with the rubber damper, the lateral displacement due to the coupled bending vibration is less influenced, because the damping effect corresponding to bending vibration displacement is obtained by means of attaching the rubber damper.

On the other hand, in 4-th order vibration component as shown in Fig. 21, the lateral displacement is larger than that of 8-th order vibration component, but lateral displacement due to coupled bending vibration does not occur remarkably. Thereforre, it is considered that the lateral displacement occurs more remarkably as the order vibration becomes higher.

Moreover, inertia mass change of the rubber damper does not influence the bending vibration of crankshaft system with the rubber damper.

9.2 On Lateral Displacement at Pin Center

Fig. 23 through 26 show the lateral displacement in the y-direction at pin center. Fig. 23 and Fig. 24 describe the amplitudes of 4-th order vibration displacement. Fig. 25 and Fig.

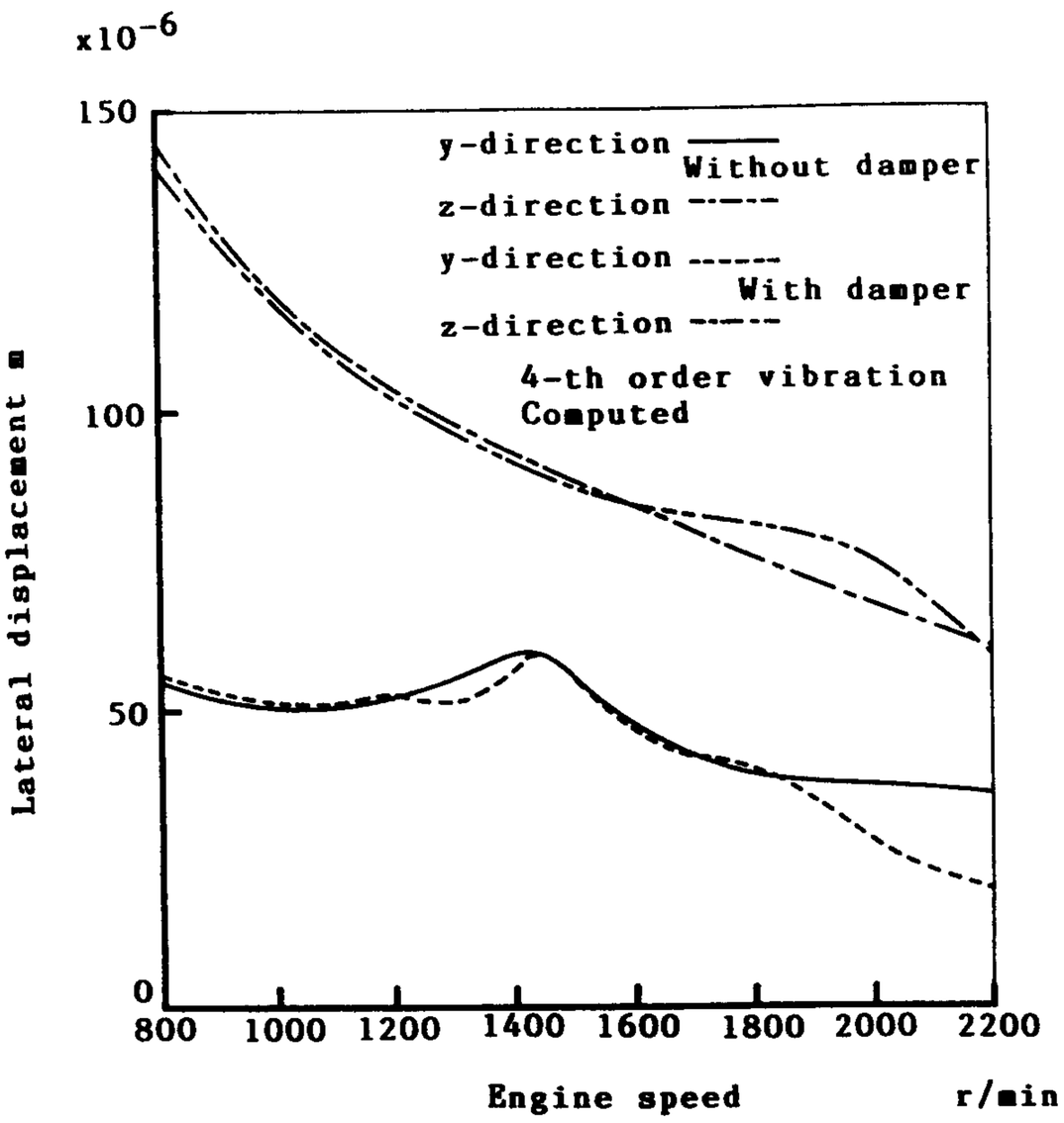

Fig. 21 Amplitude curves of lateral displacement at pulley end (4-th order vibration, computed)

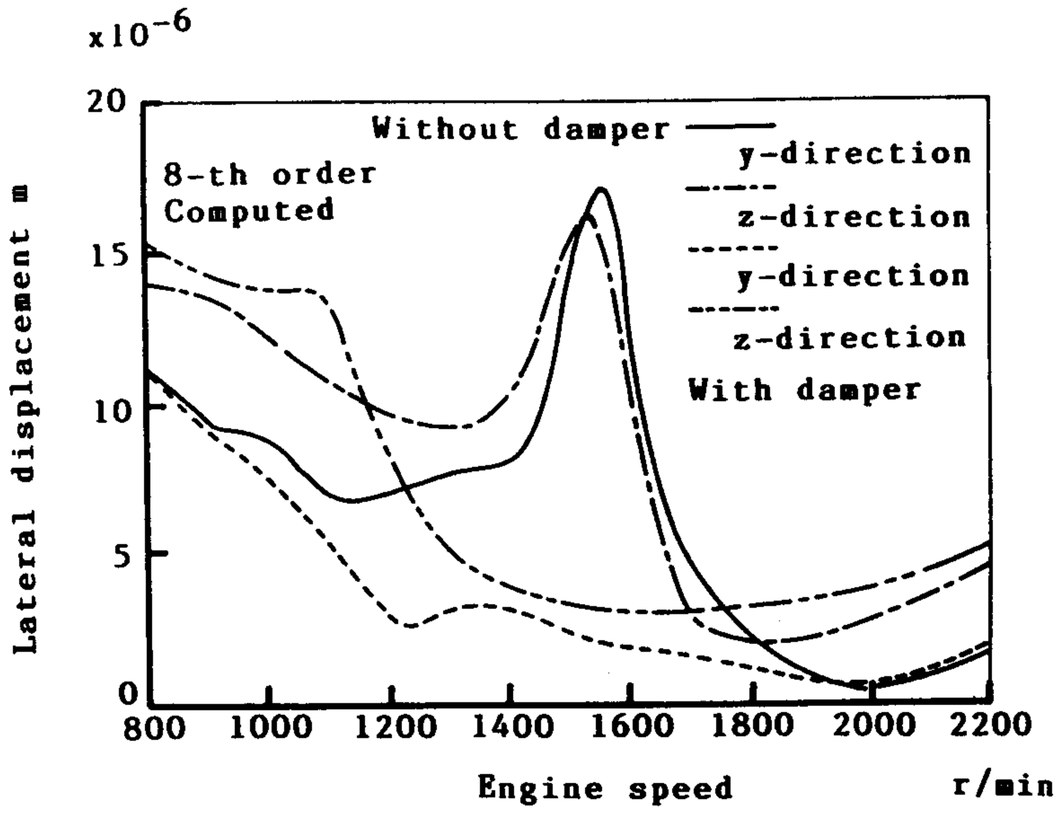

Fig. 22 Amplitude curves of lateral displacement at pulley end (8-th order vibration, computed)

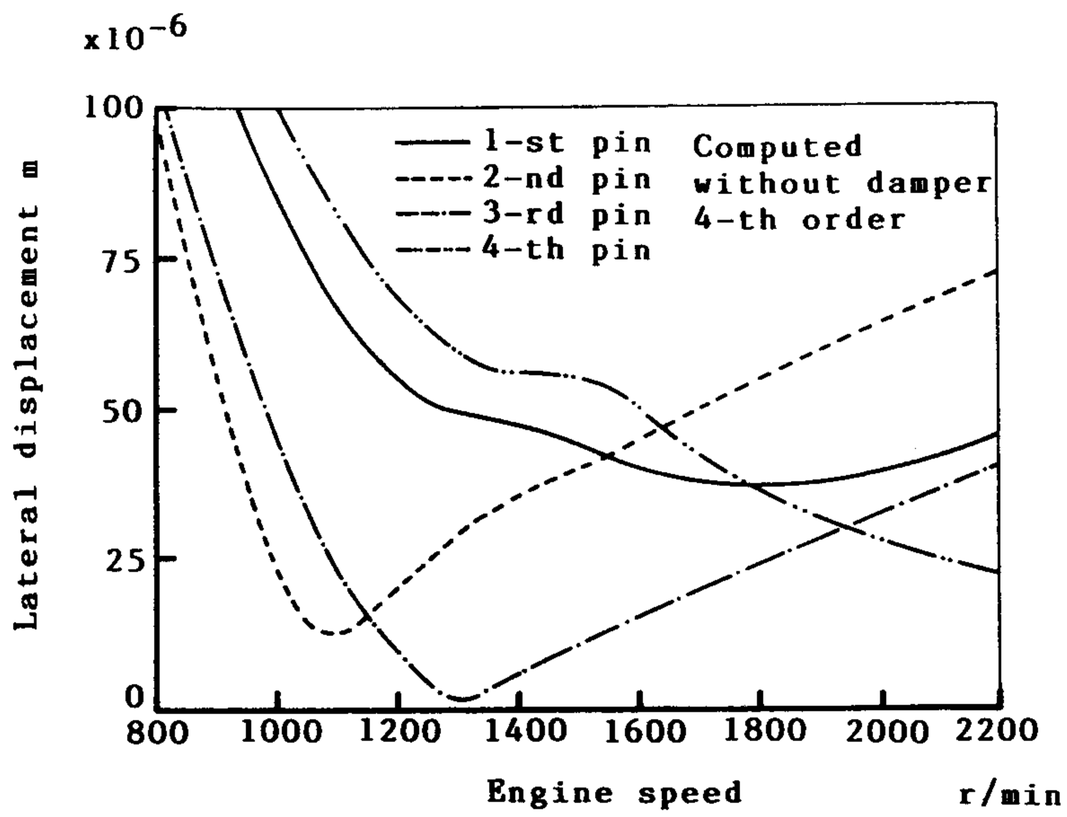

Fig. 23 Amplitude curves of lateral displacement at crank pin center (without damper, 4-th order vibration, computed)

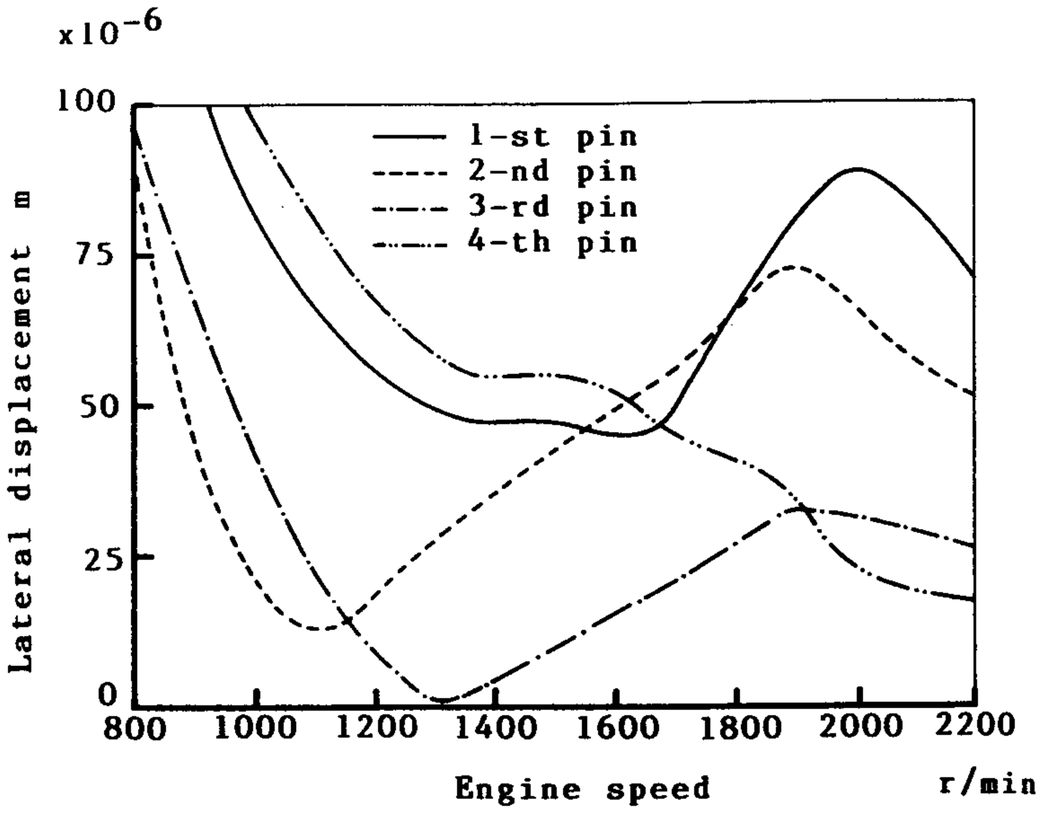

Fig. 24 Amplitude curves of lateral displacement at crank pin center (with damper, 4-th order vibration, computed)

26 describe the amplitudes of 8-th order vibration displacement. Both amplitude curves are shown in order to allow comparison with the crankshaft system without the rubber damper. The lateral displacement amplitude due to coupled bending vibration can be observed at the neighborhood of resonant revolutions of each order torsional vibration. Moreover, the resonant phenomena occur remarkably at crank throw of pulley side (1-st pin, 2-nd pin, ...in turn).

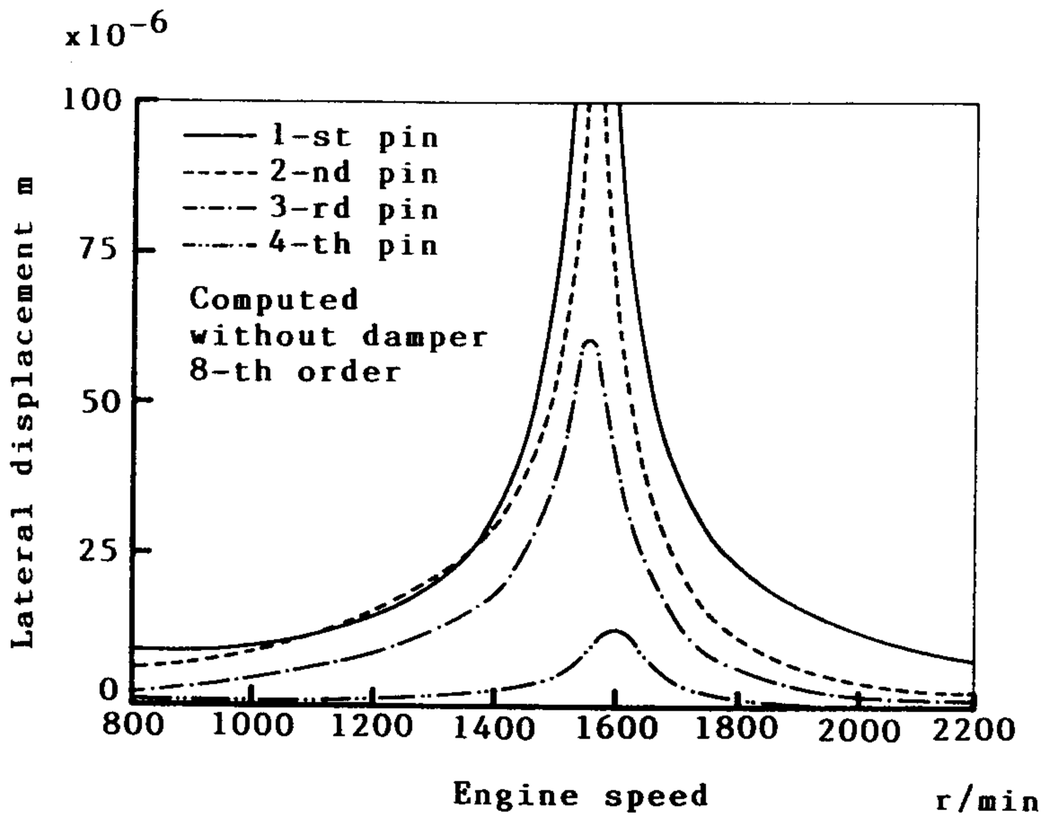

Fig. 25 Amplitude curves of lateral displacement at crank pin center (without damper, 8-th order vibration, computed)

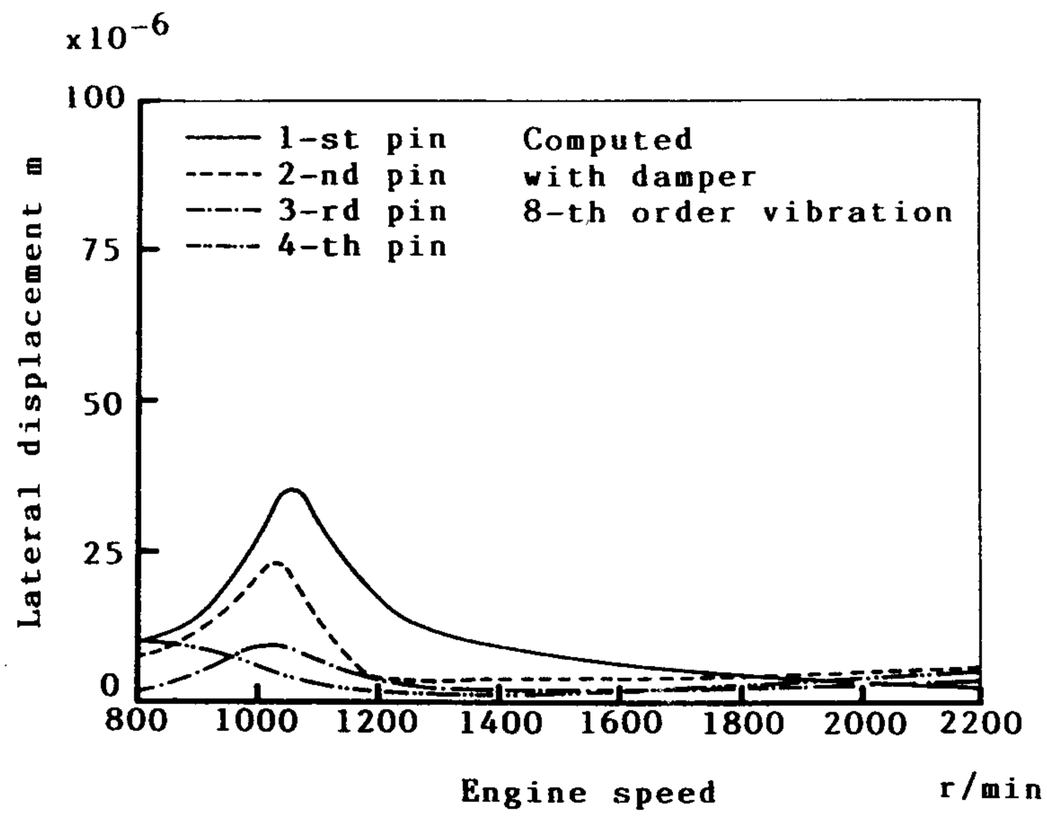

Fig. 26 Amplitude curves of lateral displacement at crank pin center (with damper, 8-th order vibration, computed)

9.3 On Bending Vibration Stress

Fig. 27 shows a computation result of bending vibration stress coupled with torsional vibration at the neighborhood of resonant revolution of 8-th order torsional vibration. The stress amplitude is not remarkable, but the bending vibraiton conditions coupled with torsional vibration can be computed. And it is inferred that the amplitudes denote different values due to each crank pin at the neighborhood of 8-th order torsional vibration.

10. Conclusion

A numerical computation by the three dimensional transfer matrix method is represented in this work. This method is applied to compute the torsional vibration displacements and stresses of a crankshaft system with a shear rubber torsional damper. The accuracy of this computation method is confirmed by comparing computed results with measured ones. Especially, in this work, the numerical vibration model of the rubber part of the rubber damper is replaced with a simple model spring-dashopt. The dynamic characteristic values to compute the rubber part of rubber damper are estimated by a three-element Maxwell model. The conclusions obtained with this numerical method are as follows;

1) The torsional vibration displacement and stress of a crankshaft system with a shear rubber torsional damper can be computed with an adequate accuracy by replacing the rubber part of rubber damper with the spring-dashpot model.

2) Then dynamic characteristic values are estimated by the complex torsional stiffness derived from the three-element Maxwell model.

3) The torsional vibration mode can be computed, so that the vibration node can be positioned more exactly.

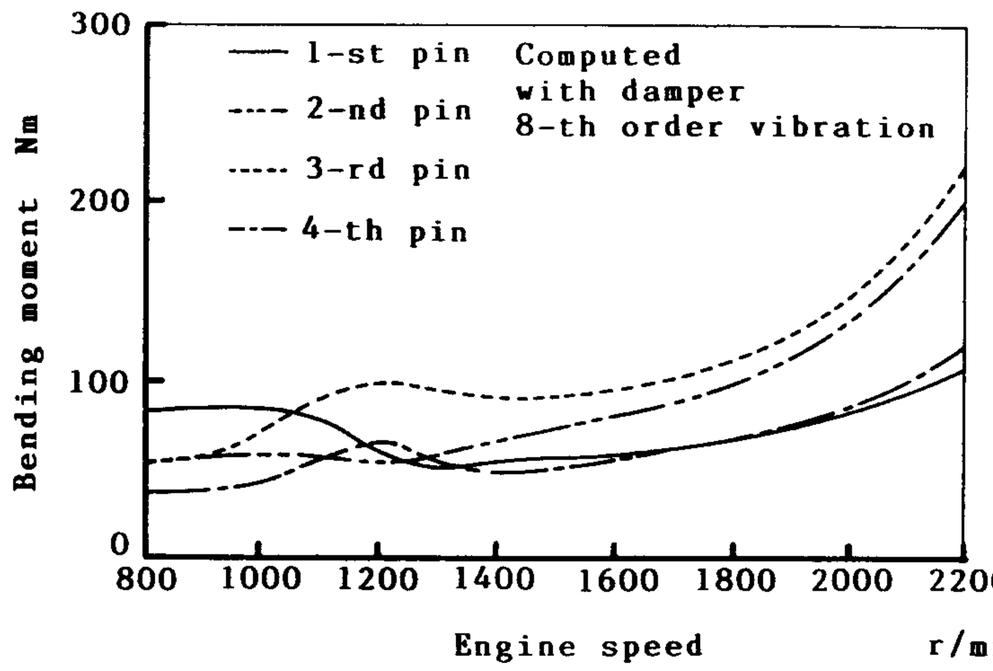

Fig. 27 Amplitude curves of bending moment at crank pin center (with damper, 8-th order vibration, computed)

4) In the crankshaft system with rubber damper, the resonant revolution of torsional vibration displacement does not necessarily coincide with the resonance of torsinal vibration stress.

5) The rebolutions at peaks of torsional stress amplitude curves per crank pin are different.

6) The bending vibration stress coupled with torsional vibration occurs at the neighborhood of resonant revolution.

11. Acknoweledgment

The SAE (Society of Automotive Engineering) International Congress and Exposition was held on 28th Feburary to 5th March 1993 at Detroit Michigan. I participated in SAE Conference and the most of this work made a presentation at the meeting. I am thankful for the financial assistance of a part of expense for participation from Faculty of Engineering of Kokushikan University.

(Received Nov. 19, 1993)

References

1) J. Hoshino, "Design for Strength of Crankshaft in Marine Diesel Engine", Journal of the M.E.S.J., Vol. 2, No. 6, 1967.
2) J. Arai, "Some Studies on Crankshaft Strength", Journal of the M.E.S.J., Vol. 4, No. 12, 1969.
3) J. Arai, "The Bending Stress Concentration factor of Solid Cranskhaft", Journal of the M.E.S.J., Vol. 9, No. 10, 1964.
4) Y. S. Park *et al.*, "Dynamic Torsional and Bending Stress Measurement from Operating Crankshaft", SAE paper, No. 860232, 1986.
5) S. Iwamoto and K. Shimoyamada *et al.*, "Vibration Analysis of Large Low-speed Marine Diesel Engine Shafting", Journal of the M.E.S.J., Vol. 24, No. 12, 1989.
6) K. Tsuda, "Vibration of Internal Combustion Engines", Science of Engines, Vil. 1, 1967.
7) K. Tsuda, "Tendency to Vibrations Study of Internal Combustion Engines", Journal of the M.E.S.J., Vol. 19, No. 8, 1974.

8) K. Wakabayashi and S. Iwamoto *et al.*, "Analysis of Vivration of Reciprocating Shaftings by the Transfer Matrix Method —The First Report: Analysis of Forced Vibration of a Crankshaft—", Bulletin of the M.E.S.J., Vol. 15, No. 3, 1980.
9) K. Wakabayashi and S. Iwamoto *et al.*, "Analysis of Vivration of Reciprocating Shaftings by the Transfer Matrix Method —The Second Report: Calculation and Comparisons with Measured Data of Torsional Vibration—", Bulletin of the M.E.S.J., Vol. 15, No. 3, 1980.
10) K. Wakabayashi and S. Iwamoto *et al.*, "Analysis of Vivration of Reciprocating Shaftings by the Transfer Matrix Method —The Third Report: Bending Vibration Stresses Excited by Torsional Vibration of Crankshafts of High Speed Small Diesel Engine—", Bulletin of the M.E.S.J., Vol. 15, No. 12, 1982.
11) K. Wakabayashi and S. Iwamoto *et al.*, "Analysis of Vivration of Reciprocating Shaftings by the Transfer Matrix Method —The Fourth Report: Torsional VibrationStress of a Crankshaft with a Ciscous Fluid Damper—", Bulletin of the M.E.S.J., Vol. 15, No. 1, 1980.
12) T. Yonezawa *et al.*, "A Study of Crankshaft Vibration Analysis of Stiffness by transfer Matrix Method—", Journal of the M.E.S.J., Vol. 20, No. 5, 1985.
13) K. Wakabayashi, K. Shimoyamada *et al.*, "The Application of a Combined Transfer Matrix Method and Finite Element Method to the Estimation of Vibration Stress of a Reciprocating Engine Crankshaft", I. Mech. E., C19/87, 1987.
14) O. Tomiyama, "Fatigue Strength and Torsional Vibration of Reciprocating Engine", CORONA Publishing Co. Ltd., 1970.
15) K. Shimoyamada, S. Iwamoto, T. Kodama *et al.*, "A Numerical Simulation Method for Vibration Stress Waveforms of Reciprocating Diesel Engine Crankshaft", Journal of the M.E.S.J., Vol. 25, No. 9, 1990.
16) K. Shimoyamada, T. Kodama, Y. Honda *et al.*, "A Numerical Analysis for Vibration Stress Waveforms of a V-Type 8 cylinder Engine Crankshaft", Bulletin of Science and Engineering Research Institute Kokushikan University, No. 3, September, 1992.
17) K. Shimoyamada, S. Iwamoto, T. Kodama *et al.*, "A Numerical Simulation Method for Vibration Stress Waveforms of High-Speed Diesel Ebgine Crankshaft System", SAE Paper, No. 910631, 1991.
18) T. Kodama, K. Shimoyamada, S. Iwamoto *et al.*, "A Numerical Analysis of Forced Torsional Vibration of Crankshaft with a Shear Type Rubber Torsional Damper by the Transfer Matrix Method —1st Report: Comparison with Computation and Measurement of Torsional Vibration Displacement—", Transaction of J.S.A.E., Vol. 23, No. 1, January, 1992.
19) Y. Honda, T. Saito, K. Kawabayashi *et al.*, "A Simulation Method for Crankshaft Torsional Vibration by Considering Dynamic Characteristcs of Rubber Dampers", SAE Paper No. 891172, 1989.
20) Y. Honda, T. Saito, K. Kawabayashi *et al.*, "An Analysis on Torsional Vibration of Crankshaft with Rubber Damper by Using Transition Metrix Method —1st Report: An Evaluation on Torsional Vibration Rubber Damper with Various Characteristics—", Transaction of J.S.A.E., No. 46, 1990.
21) T. Kodama, K. Wakabayashi, Y. Honda *et al.*, "An Analysis on Torsional Vibration of Crankshaft with Rubber Damper by Using Transition Matrix Method —2nd Report: Inference of Temperature Dependency of Rubber Damper on Torsional Vibration—", Transaction of J.S.A.E., No. 46, 1990.